Sliding Cycles of Regularized Piecewise Linear Visible–Invisible Twofolds

Renato Huzak[1] · **Kristian Uldall Kristiansen**[2]

Abstract

The goal of this paper is to study the number of sliding limit cycles of regularized piecewise linear visible–invisible twofolds using the notion of slow divergence integral. We focus on limit cycles produced by canard cycles located in the half-plane with an invisible fold point. We prove that the integral has at most 1 zero counting multiplicity (when it is not identically zero). This will imply that the canard cycles can produce at most 2 limit cycles. Moreover, we detect regions in the parameter space with 2 limit cycles.

Contents

✉ Kristian Uldall Kristiansen
  krkri@dtu.dk

1   Hasselt University, Campus Diepenbeek, Agoralaan Gebouw D, 3590 Diepenbeek, Belgium

2   Department of Applied Mathematics and Computer Science, Technical University of Denmark, 2800 Kgs. Lyngby, Denmark

Ⓑ Birkhäuser

1 Introduction

The point of departure for the present paper is planar piecewise linear (PWL) systems:

$$\dot{z} = \begin{cases} Z^+(z) \text{ for } h(z) > 0, \\ Z^-(z) \text{ for } h(z) < 0, \end{cases} \quad z = (x, y) \in \mathbb{R}^2 \tag{1}$$

where the vector-fields $Z^+ = (X^+, Y^+)$ and $Z^- = (X^-, Y^-)$ and the function $h : \mathbb{R}^2 \to \mathbb{R}$, $\nabla h \neq 0$, are each affine. The interest in such systems was perhaps first sparked by Lum and Chua [52], when they conjectured that the number of limit cycles of (1) in the continuous case, i.e. when $Z^+(z) = Z^-(z)$ for all

$$z \in \Sigma := h^{-1}(0),$$

is at most one. This conjecture, which was first proven by Freire et al. [25], led to subsequent developments [27, 31, 49, 50], where the assumption of continuity of (1) was relaxed. In such cases, the problem is to determine the maximum number of crossing limit cycles. These cycles are limit cycles of (1) that intersect Σ in discrete points z, where $Z^-(z)$ and $Z^+(z)$ point in the same direction relative to Σ; this is in contrast to so-called sliding cycles, where solutions of (1) slide (due to the Filippov convention [24]) along a subset of the discontinuity set Σ where $Z^\pm(z)$ are in oppositions relative to Σ, see Sect. 2 for further details. At present, only certain subcases of the problem have been solved, see [23, 47]. To the best of our knowledge, 3 crossing limit cycles have been realized. We also refer to [5, 7, 28, 30, 48, 51, 54] and references therein for further background on piecewise smooth systems.

Until recently, the analysis of crossing limit cycles in PWL systems was largely based upon a case-by-case analysis (see e.g. [26, 32, 33, 45, 46, 53]), depending on the type of the singularity in $h(z) < 0$ and $h(z) > 0$ and whether the singularities are virtual or not (i.e. whether they are contained within the relevant sets $h(z) \gtrless 0$). Recently, however, Carmona and Fernández-Sánchez [6] developed the foundations for a case-independent approach based upon integral representations of the Poincaré half-maps (see Sect. 2 for further details). In [9], this approach was used to show that the maximum number of crossing limit cycles is in fact uniformly bounded by 8 and in [11] the authors gave the first case-independent proof of Lum and Chua's conjecture. Finally, in [10] the uniqueness of limit cycles for sewing PWL systems (where there is no sliding) was also proven using the approach of [6].

Obviously, the interest in bounding the number of limit cycles for (1) is related to Hilbert's 16th problem [55], which seeks to bound the number of limit cycles of polynomial systems. While some progress has been made on the quadratic case [22] and on Smale's version of the problem (where the polynomial systems are restricted to being of Liénard type, see e.g. [12]), Hilbert's 16th problem remains unsolved to this day. Recently, some emphasis has been on obtaining good lower bounds on the

Fig. 1 The fast dynamics of system (2) with indication of the slow dynamics along the line of singular points $\{y = 0\}$ (blue). $\widetilde{\Gamma}_x$ is a canard cycle (Color figure online)
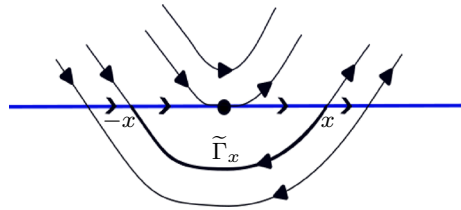
number of limit cycles (see e.g. [1, 17, 19]). A key tool in this effort has been the *slow divergence-integral*, developed by De Maesschalck, Dumortier and Roussarie, see [14–16, 20, 21], in the context of slow–fast systems and canard theory. In particular, zeros of the slow divergence-integral provide candidates for limit cycles.

Let us briefly explain the slow divergence-integral using the following smooth slow–fast system with a slow–fast Hopf/canard point [34]

$$\begin{cases} \dot{x} = y, \\ \dot{y} = xy + \epsilon \left(c - x + x^2 F(x) \right), \end{cases} \tag{2}$$

where $\epsilon \geq 0$ is a small singular parameter, $c \in \mathbb{R}$ is close to 0 and F is a smooth function. The dynamics of system (2) with $\epsilon = 0$ (often called the fast dynamics) has a line of singular points $\{y = 0\}$. For each singular point different from $(0, 0)$, the linear part of the vector field has a nonzero eigenvalue. The line is normally attracting when $x < 0$ (the nonzero eigenvalue is negative) and normally repelling when $x > 0$ (the nonzero eigenvalue is positive). Fast movement ($\epsilon = 0$) happens along parabolas $y = \frac{1}{2}x^2 + C$. We have a nilpotent singularity at $(0, 0)$ which we call a contact point between the line of singular points and the parabolas. We refer to Fig. 1.

Near normally attracting or repelling points, there are invariant manifolds asymptotic to the line of singular points, and using asymptotic expansions in ϵ we get (see [34])

$$y = \epsilon \left(-\frac{c - x + x^2 F(x)}{x} \right) + O(\epsilon^2).$$

If we now reduce the dynamics of (2) to the invariant manifolds, divide out ϵ and let $\epsilon \to 0$, we find the slow dynamics [16, Chapter 3]

$$x' = -\frac{c - x + x^2 F(x)}{x}, \quad x \neq 0.$$

For $c = 0$ the slow dynamics has a removable singularity in $x = 0$ and it points, at least near $x = 0$, from the attracting branch of $\{y = 0\}$ to the repelling branch of $\{y = 0\}$. Assume that the slow dynamics has no singularities. Then we define the slow divergence-integral associated to the line of singular points at level $c = 0$:

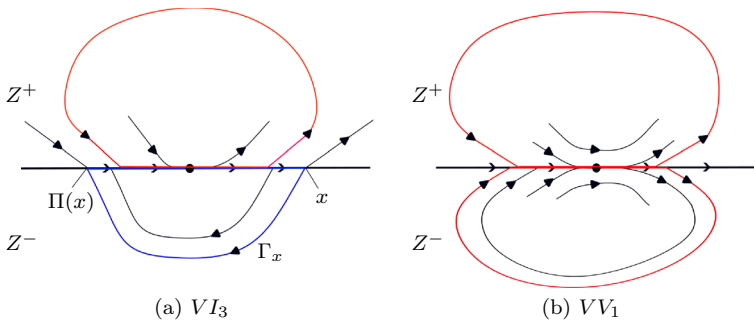$$\mathcal{I}(x) = \int_{-x}^{x} \frac{s\,ds}{1 - sF(s)}, \quad x > 0.$$

Fig. 2 Canard cycles through twofold singularities with sliding (the VI_3 case and the VV_1 case, see [44]). In this paper we study the number of limit cycles near canard cycles Γ_x (blue) located in the half-plane $y \leq 0$ with invisible fold point, in the VI_3 case. Π is the Poincaré half-map defined in Sect. 2.4. Canard cycles (red) can also appear in the half-plane with visible fold point (Color figure online)

Following [16, Chapter 5], the slow divergence-integral is the integral of the divergence of the vector field (2) for $\epsilon = 0$, computed along $\{y = 0\}$, where the variable of integration is the time variable of the slow dynamics, called the slow time and denoted τ ($d\tau = \frac{dx}{1-xF(x)}$). The function $\mathcal{I}$ plays an important role in studying the number of limit cycles of (2) produced by canard cycles. For a fixed $x > 0$, the canard cycle $\widetilde{\Gamma}_x$ is a limit periodic set at level $(\epsilon, c) = (0, 0)$ consisting of the segment $[-x, x] \subset \{y = 0\}$ and the fast orbit from $(x, 0)$ to $(-x, 0)$ (see Fig. 1). If $\mathcal{I}$ has a zero of multiplicity $l \geq 1$ at $x = x_0$, then the canard cycle $\widetilde{\Gamma}_{x_0}$ can produce at most $l + 1$ limit cycles for (ϵ, c) close to $(0, 0)$ (see e.g. [15]).

Piecewise smooth (PWS) systems (1) bear some similarities with slow–fast systems, like (2). In Fig. 2, for example, we show phase portraits for two versions (VI_3 and VV_1 in the notation of [44]) of so-called twofolds, where orbits of Z^- and Z^+ have quadratic tangencies with Σ at the same point. In Fig. 2a the fold point from "below" in terms of Z^- is "invisible" and the graphic Γ_x consists of the orbit of Z^- from $(x, 0)$ to $(\Pi(x), 0)$ and the segment $[\Pi(x), x] \subset \{y = 0\}$ (which is an orbit segment of the Filippov sliding vector-field, see Sect. 2). Γ_x is called a sliding cycle of the PWS Filippov system, but it is reminiscent of the canard cycle $\widetilde{\Gamma}_x$ associated to (2) because it contains both stable and unstable sliding portions of the discontinuity line $y = 0$; please compare Figs. 1 and 2a.

The Refs. [3, 44] show that twofolds are generically co-dimension one bifurcations in PWS systems where two fold points (quadratic tangencies) on either side collide. It can (depending on the type) also be accompanied by bifurcations of the sliding vector-field as well as bifurcations of the sliding/crossing regions.

From [56], it is known that one way to formalise the connection between (1) and slow–fast systems is through regularized PWS systems:

$$\dot{z} = Z^+(z)\phi(h(z)\epsilon^{-2}) + Z^-(z)(1 - \phi(h(z)\epsilon^{-2})), \quad z \in \mathbb{R}^2, \qquad (3)$$

where $\phi : \mathbb{R} \to \mathbb{R}$ is a smooth regularization function:

$$\phi'(s) > 0 \text{ for all } s \in \mathbb{R}, \quad \phi(s) \to \begin{cases} 1 & \text{for } s \to \infty \\ 0 & \text{for } s \to -\infty \end{cases}. \tag{4}$$

In particular, Eq. (3) has a slow manifold (the system (3) being slow–fast upon blowup $y = \epsilon^2 y_2$) for all $0 < \epsilon \ll 1$ if the associated limiting system (1) for $\epsilon = 0$ has sliding. Moreover, the reduced problem on the slow manifold precisely agrees with the Filippov convention in the singular limit $\epsilon = 0$.

In [36], the present authors showed that the number of limit cycles of (3) for $\epsilon > 0$ is unbounded when $Z^\pm$ are quadratic vector-fields. More precisely, we showed that there exist quadratic vector-fields $Z^\pm(\cdot, \lambda)$, depending smoothly on a parameter λ, such that the following statement is true: For any $k \in \mathbb{N}$ there exist a regularization function ϕ_k satisfying (4) and a continuous function $\lambda_k : [0, \epsilon_k[\to \mathbb{R}$, with $\epsilon_k > 0$, such that (3) with $Z^\pm(\cdot, \lambda_k(\epsilon))$ and $\phi = \phi_k$ has at least $k + 1$ limit cycles. The limit cycles were all sliding cycles (like Γ_x in Fig. 2a) of (1) in the singular limit $\epsilon = 0$ and they were constructed through k simple zeros of a slow divergence-integral that was associated with the so-called VI_3 twofold of PWS systems [44], see Fig. 2. In [37], the authors develop the notion of slow divergence integrals for regularized PWS systems (3) further.

The purpose of this paper is to begin the analysis of sliding cycles in regularized PWL systems. In this paper, we focus on the VI_3-case, see Fig. 2a. The VI_3-case corresponds to collision of a visible and an invisible tangencies of Z^+ and Z^- with Σ upon parameter variation and it is, following [3, 44], characterized by $Z^\pm$ being anti-collinear at the twofold and by the sliding vector-field pointing from the stable to the unstable sliding region (with nonzero speed). If we fix local coordinates such that the twofold is at the origin and $\Sigma = \{y = 0\}$, then the definition of VI_3 takes the following form:

$$\begin{cases} X^+(0,0) & > 0, \\ Y^+(0,0) & = 0, \\ \frac{\partial}{\partial x} Y^+(0,0) & > 0, \end{cases} \quad \begin{cases} X^-(0,0) & < 0, \\ Y^-(0,0) & = 0, \\ \frac{\partial}{\partial x} Y^-(0,0) & < 0, \end{cases} \tag{5}$$

and

$$\left(X^- \frac{\partial}{\partial x} Y^+ - X^+ \frac{\partial}{\partial x} Y^- \right)(0,0) > 0, \tag{6}$$

see [3, 44], and the following system

$$Z^-(x, y) = \begin{bmatrix} -1 + d^- y \\ -x + t^- y \end{bmatrix}, \quad Z^+(x, y) = \begin{bmatrix} b^+ + a_{11}^+ x + a_{12}^+ y \\ a_{21}^+ x + a_{22}^+ y \end{bmatrix},$$

with $b^+ > a_{21}^+ > 0$ and Z^- in Liénard form, is a normal form in the PWL context, see Proposition 2.1 below. VI_3 is also a bifurcation of a singularity of the sliding

vector-field (going from a saddle to a node, like the canard point of slow–fast system [43]), see [3, 44].

In this paper, we show (when the slow divergence integral is not identically zero) that the family of canard cycles $\cup_{x \in J} \Gamma_x$ for the VI_3 twofold (blue in Fig. 2a), with $J \subset \mathbb{R}_+$ being a compact interval, can produce at most 2 limit cycles of (3). This will follow from [36] and Theorem 3.1 in Sect. 3, which states that the slow divergence integral has at most 1 zero counting multiplicity in J (Remark 3 in Sect. 3). Interestingly, the proof of Theorem 3.1 uses the case-independent approach of [6] to characterize the half-maps and we relate the existence of zeros of the slow-divergence integral to crossing cycles of a sewing PWL system using [10]. We also present precise results, depending on the region of parameter space, and find that 2 sliding limit cycles can exists for (3) in cases where the singularity of Z^- is hyperbolic (saddle, focus or node). In contrast, at most one limit cycle can exists in cases where Z^- has a center or no singularities (Remark 3 and Sect. 4).

In a separate paper [35], we consider the remaining cases, including the VV_1 case (Fig. 2b). More precisely, sliding limit cycles can be produced by canard cycles detected in the half-plane with visible fold point (see red graphics in Fig. 2). We expect the existence of 3 sliding cycles in regularized PWL VI_3 and VV_1 systems.

We finally emphasize that regularized PWS systems (3) occur naturally in many different applications, including in models of friction (see [2, 4, 13, 41]). Moreover, there has recently been a desire to understand how PWS phenomena (folds, grazing, boundary equilibria [44]) unfold in the smooth version [3, 38–40, 42]. For this purpose methods from Geometric Singular Perturbation Theory (GSPT) and blowup have been refined to deal with resolving the special singular limit of (3), see [36, 40, 41].

The paper is organized as follows: In Sect. 2, we first review some basic concepts of Filippov PWS systems and present a normal form for the PWL VI_3-case, see Sects. 2.1 and 2.2. In Sect. 2.3, we define our regularized PWL VI_3 twofold model and introduce the notion of slow divergence integral. Finally, in Sect. 2.4 we present some results on a Poincaré half-map based on the work of [6]. Subsequently, we then state our main result about the upper bound for the number of zeros of the slow divergence integral, Theorem 3.1 in Sect. 3. During the reviewing process, an anonymous referee provided an alternative proof of Theorem 3.1, available in Sect. 3, that does not distinguish between cases depending on the spectrum of the linear systems (see also Remark 2), but rather uses the integral characterizations of Poincaré half-maps [6] (see Sect. 2.4), and apply results of [8, 10]. In Sect. 4, we proceed to deal with the different cases (saddle, focus, proper and improper node, etc.) separately; collectively, these results also prove Theorem 3.1. In each case, we state precise cyclicity results for canard cycles, depending on the region of parameter space (see Theorems 4.1, 4.3, 4.5, 4.7 and 4.9 in Sect. 4); for more details about the definition of cyclicity, we refer the reader to Sect. 2.3. In particular, we detect regions in the parameter space with 2 sliding limit cycles.
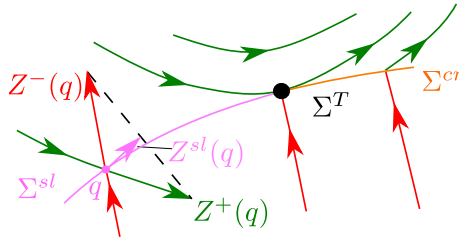
Fig. 3 Illustration of a PWS visible fold Σ^T, that locally divides Σ into a crossing set Σ^{cr} (orange) and a sliding set Σ^{sl} (pink, stable in the present case). On Σ^{sl} we assign Filippov's sliding vector-field Z^{sl}, which is defined as the convex combination of $Z^{\pm}(q)$ that is tangent to Σ at $q \in \Sigma$ (Color figure online)

2 Background

2.1 Filippov PWS Systems

In the following, we review the most basic concepts of PWS systems. For this purpose, we will follow [36, Section 2] (which is based upon [3, 18, 44]). Notice that henceforth we write $\mathcal{L}_{Z^{\pm}}(h) := \nabla h \cdot Z^{\pm}$ for the Lie-derivative of h in the direction $Z^{\pm}$. We also write $(\mathcal{L}_{Z^{\pm}})^2(h) := \mathcal{L}_{Z^{\pm}}(\mathcal{L}_{Z^{\pm}}(h))$.

The discontinuity set $\Sigma = \{h(z) = 0\}$ of (1) is frequently called the switching manifold [18, 29] and it is divided into three disjoint sets $\Sigma = \Sigma^{cr} \cup \Sigma^{sl} \cup \Sigma^T$ characterized in the following way:

(1) The subset $\Sigma^{cr} \subset \Sigma$ consisting of all points $q \in \Sigma$ where

$$\mathcal{L}_{Z^+}(h)(q)\mathcal{L}_{Z^-}(h)(q) > 0,$$

is called "crossing", see Fig. 3 (orange).
(2) The subset $\Sigma^{sl} \subset \Sigma$ consisting of all points $q \in \Sigma$ where

$$\mathcal{L}_{Z^+}(h)(q)\mathcal{L}_{Z^-}(h)(q) < 0,$$

is called "sliding". It is said to be stable (resp. unstable) if $\mathcal{L}_{Z^+}(h)(q) < 0$ and $\mathcal{L}_{Z^-}(h)(q) > 0$ (resp. $\mathcal{L}_{Z^+}(h)(q) > 0$ and $\mathcal{L}_{Z^-}(h)(q) < 0$). Figure 3 illustrates (in pink) stable sliding (unstable sliding can be obtained by reversing the arrows).
(3) The subset $\Sigma^T \subset \Sigma$ consisting of all points $q \in \Sigma$ where either $\mathcal{L}_{Z^+}(h)(q) = 0$ or $\mathcal{L}_{Z^-}(h)(q) = 0$ is called the set of tangency points. If $q \in \Sigma^T$ and $\mathcal{L}_{Z^+}(h)(q) = 0$ then q is called a tangency point from above. Tangency points from below are defined similarly. Finally, q is a double tangency point if it is tangency point from above and from below.

Along Σ^{cr}, trajectories can be extended from Z^+ to Z^- or from Z^- to Z^+ by concatenating orbits of Z^+ and Z^-. In contrast, trajectories of $Z^{\pm}$ reach Σ^{sl} in finite time and to be able to continue trajectories a vector-field has to be defined along Σ^{sl}. The most common way to do this is by using the Filippov convention, where the *sliding*

vector-field Z^{sl} is assigned on Σ^{sl}:

$$Z^{sl}(q) = Z^+(q)p(q) + Z^-(q)(1 - p(q)), \quad p(q) := \frac{-\mathcal{L}_{Z^-}(h)}{\mathcal{L}_{Z^+}(h) - \mathcal{L}_{Z^-}(h)}(q), \quad (7)$$

for $q \in \Sigma^{sl}$, see Fig. 1. In this way, one can define a forward solution and a backward solution through any point, see [24, 44]. These solutions are (clearly) not unique in general, but this allows us to define ω and α-limit sets. The choice (7) is motivated by examples [18], but importantly it also relates to the $\epsilon \to 0$ limit of (3), see [36] and Sect. 2.3 below.

Frequently, we will suppose that $h(x, y) = y$, which is without loss of generality in the PWL case (and locally in the nonlinear case). In this case, $Z^{sl} = (X^{sl}, 0)$ which defines X^{sl} (a one-dimensional vector-field on $\Sigma^{sl} \subset \{y = 0\}$).

We further classify the points in Σ^T as follows (see also [18]):

(4) A point $q \in \Sigma^T$ is a fold point from "above" if the orbit of $Z^+(\cdot)$ through q has a quadratic tangency with Σ at q, i.e.

$$\begin{cases} Z^+(q) & \neq 0, \\ \mathcal{L}_{Z^+}(h)(q) & = 0, \\ (\mathcal{L}_{Z^+})^2(h)(q) & \neq 0. \end{cases}$$

We define a fold point from "below" in terms of Z^- in a similar way.

(5) A fold point $q \in \Sigma^T$ from "above" is said to be visible, if the orbit of $Z^+(\cdot)$ through q is contained within $y > 0$ in neighborhood of q. It is said to be invisible otherwise. In terms of Lie-derivatives, we clearly have $(\mathcal{L}_{Z^+})^2(h)(q) > 0$ iff q satisfying $Z^+(q) \neq 0$ and $\mathcal{L}_{Z^+}(h)(q) = 0$ is visible. Fold points from below are classified in a similar way. In particular, $(\mathcal{L}_{Z^-})^2(h)(q) < 0$ iff q satisfying $Z^-(q) \neq 0$ and $\mathcal{L}_{Z^-}(h)(q) = 0$ is visible.

The fold point illustrated in Fig. 3 (black dot) is visible from above.

2.2 Twofolds and a Normal Form for the PWL VI_3-Case

Now, we finally arrive at the concept of twofolds in PWS systems. These are double tangency points that are fold points for both vector-fields and play the role of canard points in the analysis of (3), see [36].

(6) A twofold $q \in \Sigma^T$ is a point with quadratic tangencies from above *and* from below. In terms of Lie-derivatives we have:

$$\begin{cases} Z^\pm(q) & \neq 0, \\ \mathcal{L}_{Z^\pm}(h)(q) & = 0, \\ (\mathcal{L}_{Z^\pm})^2(h)(h)(q) & \neq 0, \end{cases}$$

with these equations understood to hold for *both* $\pm$.

(7) A twofold is said to be visible–visible, visible–invisible, invisible–invisible accord-
ing to the "visibility" of the fold from above and below, respectively, see item (5)
above.

The paper [44] gave a characterization of twofolds. There are seven different cases,
two cases of visible–visible (called $VV_{1,2}$), three cases of visible–invisible ($VI_{1,2,3}$),
and finally two cases of invisible–invisible ($II_{1,2}$). The different subcases (of visible–
visible, visible–invisible and invisible–invisible) are determined by (a) whether there
is sliding (VV_1, VI_2, VI_3 and II_1) or not (VV_2, VI_1 and II_2), and (if there is sliding:)
by (b) the direction of sliding flow and finally (c) whether the unfolding leads to
singularities on Σ^{sl} of the sliding vector-field, see also [42, Fig. 2]. In the present
paper, we focus on the VI_3-case which we characterize in the following result.

Proposition 2.1 *Consider a PWL system* (1) *with* $h(z) = y$ *and* $Z^\pm$ *affine, having a*
VI_3 *twofold at the origin, i.e.* $Z^\pm = (X^\pm, Y^\pm)$ *satisfy* (5) *and* (6). *Then there exists*
an invertible affine map $\Phi : (x, y) \mapsto (\tilde{x}, \tilde{y})$ *such that* $\widetilde{Z}^\pm := \Phi^*(Z^\pm)$ *are given by*

$$\widetilde{Z}^-(\tilde{x}, \tilde{y}) = \begin{bmatrix} -1 + d^-\tilde{y} \\ -\tilde{x} + t^-\tilde{y} \end{bmatrix}, \quad \widetilde{Z}^+(\tilde{x}, \tilde{y}) = \begin{bmatrix} b^+ + a_{11}^+\tilde{x} + a_{12}^+\tilde{y} \\ a_{21}^+\tilde{x} + a_{22}^+\tilde{y} \end{bmatrix}. \tag{8}$$

Here $b^+ > a_{21}^+ > 0$, $\Sigma^{sl} =\,]-\infty, 0[\cup\,]0, \infty[$, $\Sigma^T = \{0\}$,

$$t^- = \mathrm{tr}(DZ^-), \quad d^- = \det(DZ^-),$$

and

$$\widetilde{X}^{sl}(x) = \frac{1}{1 + a_{21}^+} \left(b^+ - a_{21}^+ + a_{11}^+ x \right).$$

Proof We write

$$Z^\pm(z) = A^\pm z + b^\pm,$$

with $A^\pm = [a_{ij}^\pm]$ and $b^\pm = [b_1^\pm, b_2^\pm]^T$. Then the conditions (5) and (6) become

$$\begin{cases} b_1^+ > 0, \\ b_2^+ = 0, \\ A_{21}^+ > 0, \end{cases} \quad \begin{cases} b_1^- < 0, \\ b_2^- = 0, \\ A_{21}^- < 0, \end{cases}$$

and

$$b_1^- a_{21}^+ - b_1^+ a_{21}^- > 0. \tag{9}$$

Since $a_{21}^- \neq 0$, we can transform Z^- into a Liénard form $\widetilde{Z}^-$ with $\widetilde{a}_{11}^- = 0$ using an y-fibered isomorphism defined by

$$(x, y) \mapsto \tilde{x} = x - \frac{a_{11}^-}{a_{21}^-} y.$$

Dropping the tildes, we can then subsequently apply the scalings

$$(x, y) \mapsto \begin{cases} \tilde{x} &= |b_1^-|^{-1} x, \\ \tilde{y} &= |b_1^-|^{-1} |a_{21}^-|^{-1} y \end{cases}$$

This gives $\widetilde{Z}^\pm(\tilde{z}) = \widetilde{A}^\pm \tilde{z} + \tilde{b}^\pm$ with

$$\widetilde{A}^+ = [\tilde{a}_{ij}], \quad \tilde{b}^+ = \begin{bmatrix} \tilde{b}_1^+ \\ 0 \end{bmatrix}, \quad \widetilde{A}^- = \begin{bmatrix} 0 & \det(A^-) \\ -1 & \operatorname{tr}(A^-) \end{bmatrix}, \quad \tilde{b}^- = \begin{bmatrix} -1 \\ 0 \end{bmatrix},$$

Setting $a_{21}^+ := \widetilde{a}_{21}^+$, $b^+ := \tilde{b}_1^+$, Eq. (9) becomes $b^+ - a_{21}^+ > 0$. The expression for $\widetilde{X}^{sl}$ follows easily from (7). This completes the proof. □

In the rest of this paper, when we refer to (8), we use $Z^\pm$, X^{sl} instead of $\widetilde{Z}^\pm$, $\widetilde{X}^{sl}$.

2.3 Regularized PWL VI_3 Twofold and the Slow Divergence Integral

We now consider (3) with $h(x, y) = y$ in the form

$$\dot{z} = Z^+(z, \lambda) \phi(y\epsilon^{-2}) + Z^-(z, \lambda)(1 - \phi(y\epsilon^{-2})), \tag{10}$$

where $0 < \epsilon \ll 1$, $\lambda \sim 0 \in \mathbb{R}$, $Z^\pm(\cdot, \lambda) = (X^\pm(\cdot, \lambda), Y^\pm(\cdot, \lambda))$ are planar affine vector-fields, depending smoothly on a parameter λ, and $Z^\pm(\cdot, 0) = Z^\pm(\cdot)$, with $Z^\pm(\cdot)$ defined in (8). We add the following technical assumptions on ϕ.

(A1) The function ϕ has the following asymptotics when $s \to \pm\infty$:

$$\phi(s) \to \begin{cases} 1 & \text{for } s \to \infty, \\ 0 & \text{for } s \to -\infty. \end{cases}$$

(A2) The function ϕ is strictly monotone, i.e., $\phi'(s) > 0$ for all $s \in \mathbb{R}$.
(A3) The function ϕ is smooth at $\pm\infty$ in the following sense: Each of the functions

$$\phi_+(s) := \begin{cases} 1 & \text{for } s = 0, \\ \phi(s^{-1}) & \text{for } s > 0, \end{cases}, \quad \phi_-(s) := \begin{cases} \phi(-s^{-1}) & \text{for } s > 0, \\ 0 & \text{for } s = 0, \end{cases}$$

are smooth at $s = 0$.

Assumption (A3) means that (10) is a regular perturbation of $Z^+(\cdot, \lambda)$ or $Z^-(\cdot, \lambda)$ outside any fixed neighborhood of $y = 0$, see [36]. Moreover, it is well-known (see [56] and [36, Theorem 2.2]) that once Assumption (A2) holds, sliding in (8) implies existence of local invariant manifolds for (10), which carry a reduced flow that is a regular perturbation of $\dot{x} = X^{sl}(x)$, with X^{sl} given in Proposition 2.1:

$$X^{sl}(x) = \frac{1}{1 + a_{21}^+} \left(b^+ - a_{21}^+ + a_{11}^+ x \right). \tag{11}$$

When $a_{11}^+ \neq 0$, X^{sl} has a simple zero

$$x^* = -\frac{b^+ - a_{21}^+}{a_{11}^+} \neq 0, \tag{12}$$

and when $a_{11}^+ = 0$, $X^{sl}(x)$ is positive for all $x \in \mathbb{R}$.

The following assumption plays an important role when we study the existence and number of sliding limit cycles of (10), see [36].

(A4) We assume that

$$\frac{\partial}{\partial \lambda} Y^- \frac{\partial}{\partial x} Y^+ \neq \frac{\partial}{\partial \lambda} Y^+ \frac{\partial}{\partial x} Y^- \tag{13}$$

at $(z, \lambda) = (0, 0)$.

Let us explain the meaning of Assumption (A4). The fold point $(x, y) = (0, 0)$ from above and below is persistent to smooth perturbations of (8). Indeed, The Implicit Function Theorem and (5) imply the existence of smooth λ-families of fold points $z_+ = (x_+(\lambda), 0)$ from above in terms of $Z^+(\cdot, \lambda)$ and fold points $z_- = (x_-(\lambda), 0)$ from below in terms of $Z^-(\cdot, \lambda)$, for $\lambda \sim 0$, with $x_\pm(0) = 0$. If we assume non-zero velocity of the collision between z_+ and z_- for $\lambda = 0$ at the origin $z = 0$:

$$x_+'(0) - x_-'(0) = \left(-\frac{\frac{\partial}{\partial \lambda} Y^+}{\frac{\partial}{\partial x} Y^+} + \frac{\frac{\partial}{\partial \lambda} Y^-}{\frac{\partial}{\partial x} Y^-} \right) (0, 0) \neq 0,$$

then we get (13).

Following [36, Section 3], to study the existence and number of sliding limit cycles of (10) produced by the canard cycle Γ_x (Fig. 2a) for $(\epsilon, \lambda) \sim (0, 0)$, we use the slow divergence integral associated to the segment $[\Pi(x), x]$ at level $\lambda = 0$:

$$I(x) = \int_{\Pi(x)}^{x} \frac{(Y^+ - Y^-)^2}{X^- Y^+ - X^+ Y^-} (u, 0, 0) \phi' \left(\phi^{-1} \left(\frac{-Y^-}{Y^+ - Y^-} (u, 0, 0) \right) \right) du, \tag{14}$$

for $x > 0$. See (3.1) in [36]. Now, if we use (8), then (14) becomes

$$I(x) = (1 + a_{21}^+) \phi' \left(\phi^{-1} \left(\frac{1}{1 + a_{21}^+} \right) \right) \int_{\Pi(x)}^{x} \frac{u \, du}{X^{sl}(u)}. \tag{15}$$

Notice that $I(0) = 0$ and that the expression in front of the integral in (15) is positive; roots of I are therefore independent of the regularization function, see Remark 1. The domain of I is a subset of the domain of Π (Sect. 2.4) and it depends on the location of x^* defined in (12). More precisely, the domain of I is the biggest subset $[0, \mu[$ ($\mu > 0$ or $\mu = +\infty$) of the domain of Π such that the sliding vector field X^{sl} given in (11) is positive on $[\Pi(x), x]$, for all $x \in [0, \mu[$. It should be clear that the domain of I is equal to the domain of Π when $a_{11}^+ = 0$. For more details see later sections.

Remark 1 As emphasized by (15), in the PWL case the ϕ-dependent term of the integrand of I in (14) is a constant and can therefore go outside the integration. In this sense, our analysis in the PWL case will be independent of the regularization function. This is in contrast to the general case, see [36]. There we constructed an arbitrary number of limit cycles by varying ϕ, even in the case where Z^- is affine and Z^+ is quadratic.

We assume that

$$\lambda = \epsilon \widetilde{\lambda}$$

where $\widetilde{\lambda} \sim 0$. We denote by $\mathrm{Cycl}(\Gamma_{x_0})$ the cyclicity of the canard cycle Γ_{x_0} inside (10), for $x_0 \in]0, \mu[$. More precisely, we say that the cyclicity of Γ_{x_0} inside (10) is bounded by $N \in \mathbb{N}$ if there exist $\epsilon_0 > 0$, $\delta_0 > 0$ and a neighborhood $\mathcal{U}$ of 0 in the $\widetilde{\lambda}$-space such that (10) has at most N limit cycles, lying within Hausdorff distance δ_0 of Γ_{x_0}, for all $(\epsilon, \widetilde{\lambda}) \in]0, \epsilon_0] \times \mathcal{U}$. We call the smallest N with this property the cyclicity of Γ_{x_0} and denote it by $\mathrm{Cycl}(\Gamma_{x_0})$.

We define $\mathrm{Cycl}(\cup_{x \in J} \Gamma_x)$ in a similar way, where $J = [\theta, \mu - \theta]$ (resp. $J = [\theta, \frac{1}{\theta}]$) for $\mu > 0$ (resp. $\mu = +\infty$), with any small and fixed $\theta > 0$.

The following theorem is a direct consequence of [36].

Theorem 2.2 *Consider* (10) *and suppose that Assumptions* (A1) *through* (A4) *are satisfied. Then the following statements are true.*

1. *If $I(x_0) < 0$ (resp. $I(x_0) > 0$), then $\mathrm{Cycl}(\Gamma_{x_0}) = 1$ and the limit cycle is hyperbolic and attracting (resp. repelling) when it exists. Moreover, if I has no zeros in $]0, \mu[$, then $\mathrm{Cycl}(\cup_{x \in J} \Gamma_x) = 1$.*
2. *If I has a zero of multiplicity $l \geq 1$ at $x = x_0$, then $\mathrm{Cycl}(\Gamma_{x_0}) \leq l + 1$. When I has at most $l \geq 1$ zeros in $]0, \mu[$, counting multiplicity, then we have $\mathrm{Cycl}(\cup_{x \in J} \Gamma_x) \leq l + 1$.*
3. *Suppose that I has exactly $l \geq 1$ simple zeros $x_1 < \cdots < x_l$ in $]0, \mu[$. If $x_{l+1} \in]x_l, b[$, then there is a smooth function $\widetilde{\lambda} = \widetilde{\lambda}_c(\epsilon)$, with $\widetilde{\lambda}_c(0) = 0$, such that (10) with $Z^\pm(\cdot, \epsilon \widetilde{\lambda}_c(\epsilon))$ has $l + 1$ periodic orbits $\mathcal{O}_1^\epsilon, \ldots, \mathcal{O}_{l+1}^\epsilon$, for each $\epsilon \sim 0$ and $\epsilon > 0$. The periodic orbit $\mathcal{O}_i^\epsilon$ is isolated, hyperbolic and Hausdorff close to the canard cycle Γ_{x_i}, for each $i = 1, \ldots, l + 1$.*

Proof Statements 1 and 2 follow from [36, Proposition 3.2], and Statement 3 follows from [36, Theorem 3.1]. □

2.4 Poincaré Half-Map

In this section, we focus on Z^- defined in (8) (remember we drop the tildes). The study of the transition map (often called Poincaré half-map) from $x > 0$, $y = 0$ to $x < 0$, $y = 0$ by following the orbits of Z^- in forward time can be found in [6]. We denote by Π the Poincaré half-map (Fig. 2a). From [6, Theorem 8] and [6, Theorem 19] it follows that we can use an integral characterization for the Poincaré half-map Π:

$$\int_{\Pi(x)}^{x} \frac{-u\,du}{V(u)} = 0, \tag{16}$$

where

$$V(x) = d^- x^2 - t^- x + 1.$$

Notice that V is related to the characteristic polynomial associated with Z^-:

$$P(\lambda) = \lambda^2 - t^- \lambda + d^-,$$

by

$$V(u) = u^2 P(u^{-1}),$$

for $u \neq 0$. From this, it can be easily seen that the following lemma holds.

Lemma 2.3 *The following statements are true.*

1. *If $d^- \neq 0$, then Z^- defined in (8) has a singularity at $(x, y) = (\frac{t^-}{d^-}, \frac{1}{d^-})$ with eigenvalues*

$$\varkappa_\pm = \frac{t^- \pm \sqrt{(t^-)^2 - 4d^-}}{2}. \tag{17}$$

2. *If $d^- \neq 0$ and $(t^-)^2 - 4d^- \geq 0$, then the invariant affine eigenline corresponding to the eigenvalue $\varkappa_\pm$ in (17) is given by*

$$x = \varkappa_\mp y + \frac{1}{\varkappa_\mp}, \tag{18}$$

and it intersects the x-axis at the zero $x = \frac{1}{\varkappa_\mp}$ of the polynomial V.

3. *If $d^- = 0$ and $t^- \neq 0$, then the line*

$$x = t^- y + \frac{1}{t^-} \tag{19}$$

is invariant w.r.t. Z^-. Moreover, the line intersects the $x-$axis at the zero $x = \frac{1}{t^-}$ of V.

We denote by x_L and x_R the zeros of V in Lemma 2.3:

$$x_L, \ x_R = \frac{1}{\varkappa_\pm}, \tag{20}$$

where we assume that $x_L < x_R$ if $x_L \neq x_R$.

The set $\Gamma_x \cup \text{Int}(\Gamma_x)$ belongs to the class (S_0) defined in [6] (that is, $\Gamma_x \cup \text{Int}(\Gamma_x)$ contains no singularities of Z^-). For more details we refer to Sects. 4.2–4.4, Appendices A and B. The Poincaré half-map Π can be extended to $\Pi(0) = 0$ and it is analytic in its domain of definition (see [6]). The following discussion is based on Lemma 2.3. If $(t^-)^2 - 4d^- < 0$, then Z^- has a focus or center in $\{y > 0\}$, and the domain of Π is $[0, +\infty[$ and the image of Π is $]-\infty, 0]$ (Fig. 10 in Sect. 4.4 and Fig. 12 in Appendix A). When $d^- < 0$, Z^- has a hyperbolic saddle in $\{y < 0\}$ and the stable (resp. unstable) straight manifold of the saddle intersects the x-axis at $x = x_R > 0$ (resp. $x = x_L < 0$). In this case the domain of Π is $[0, x_R[$ and the image of Π is $]x_L, 0]$ (Fig. 4 and Sect. 4.2). When Z^- has a hyperbolic node in $\{y > 0\}$ with distinct eigenvalues ($d^- > 0$ and $(t^-)^2 - 4d^- > 0$), then two straight-line solutions corresponding to the eigenvalues intersect the x-axis at $x = x_L$ and $x = x_R$ with $0 < x_L < x_R$ or $x_L < x_R < 0$. If $0 < x_L < x_R$ (resp. $x_L < x_R < 0$), then the domain of Π is $[0, x_L[$ (resp. $[0, +\infty[$) and the image of Π is $]-\infty, 0]$ (resp. $]x_R, 0]$). We refer to Fig. 6 and Sect. 4.3. System Z^- may have a hyperbolic node in $\{y > 0\}$ with repeated eigenvalues ($d^- > 0$ and $(t^-)^2 - 4d^- = 0$). In this case we have one straight-line solution (corresponding to the eigenvalue) which intersects the x-axis at $x = x_R \neq 0$. If $x_R > 0$ (resp. $x_R < 0$), then the domain of Π is $[0, x_R[$ (resp. $[0, +\infty[$) and the image of Π is $]-\infty, 0]$ (resp. $]x_R, 0]$). If Z^- has no singularities ($d^- = 0$), then there exists an invariant line intersecting the x-axis at $x = \frac{1}{t^-}$ ($t^- \neq 0$) or orbits of Z^- are parabolas $y = \frac{1}{2}x^2 + c$ ($t^- = 0$). In the former case, the domain and image of Π are respectively $[0, \frac{1}{t^-}[$ and $]-\infty, 0]$ if $t^- > 0$ or $[0, +\infty[$ and $]\frac{1}{t^-}, 0]$ if $t^- < 0$, whereas in the latter case the domain and image of Π are respectively $[0, +\infty[$ and $]-\infty, 0]$. We refer to Fig. 13 and Appendix B.

The function V is positive on the domain and image of Π. Using (16) we get

$$\Pi'(x) = \frac{x V(\Pi(x))}{\Pi(x) V(x)}. \tag{21}$$

We have $\Pi' < 0$ and $\Pi'(0) = -1$.

3 Number of Zeros of the Slow Divergence Integral

Recall that the slow divergence integral I is given by (15). Our goal is to study the number of zeros (counting multiplicity) of I in $]0, \mu[$. We show that I is either identically zero or has at most 1 zero (counting multiplicity) in $]0, \mu[$. We define the following

two quantities (see [8, Theorem 1]):

$$\xi_0 = -\frac{a_{11}^+ + t^-(b^+ - a_{21}^+)}{\sqrt{b^+ - a_{21}^+}} \quad \text{and} \quad \xi_\infty = -\frac{(a_{11}^+)^2 d^-}{b^+ - a_{21}^+}. \tag{22}$$

Theorem 3.1 *If $\xi_0 \neq 0$ or $\xi_\infty \neq 0$, then I has at most 1 zero counting multiplicity in $]0, \mu[$. If $\xi_0 = \xi_\infty = 0$, then I is identically zero.*

Remark 2 The result follows from our case-by-case analysis in Sect. 4, but in the reviewing process an anonymous referee made us aware of [10, Theorem A] and a connection between zeros of the slow-divergence integral and a sewing PWL system, see (23). This leads to a more elegant proof of Theorem 3.1, which we include below.

Proof We first assume that $\xi_0 \neq 0$ or $\xi_\infty \neq 0$ and prove that the slow divergence integral I has at most one zero in $]0, \mu[$ (counting its multiplicity). Equivalently, we must prove that the function

$$\bar{I}(x) = \int_{\Pi_-(x)}^x \frac{-u\, du}{b^+ - a_{21}^+ + a_{11}^+ u}$$

has a at most one zero in $]0, \mu[$ (counting its multiplicity), where $b^+ > a_{21}^+ > 0$ and Π_- (called Π in Sect. 2.4) is the forward Poincaré half-map of the linear system

$$\begin{cases} \dot{x} = -1 + d^- y, \\ \dot{y} = -x + t^- y, \end{cases}$$

associated to the Poincaré section $\{y = 0\}$.

As stated in [6] (see also [8, 10]), it is clear that (for $b^+ > a_{21}^+$) the backward Poincaré half-map Π_+ of the linear system

$$\begin{cases} \dot{x} = \sqrt{b^+ - a_{21}^+}, \\ \dot{y} = -x + \dfrac{a_{11}^+}{\sqrt{b^+ - a_{21}^+}} y, \end{cases}$$

associated to the Poincaré section $\{y = 0\}$, is given by the integral characterization

$$\int_{\Pi_+(x)}^x \frac{-u\, du}{b^+ - a_{21}^+ + a_{11}^+ u} = 0.$$

Therefore, the slow divergence integral I (or, equivalently, $\bar{I}$) has a zero if and only if the sewing PWL system

$$\begin{cases} \dot{x} = -1 + d^- y, \\ \dot{y} = -x + t^- y, \end{cases} \quad \text{if } y < 0, \qquad \begin{cases} \dot{x} = \sqrt{b^+ - a_{21}^+}, \\ \dot{y} = -x + \dfrac{a_{11}^+}{\sqrt{b^+ - a_{21}^+}} y, \end{cases} \quad \text{if } y > 0, \tag{23}$$

has a crossing periodic orbit. From [10, Theorem A] it follows that system (23) has at most one isolated crossing periodic orbit (that is, one limit cycle) and this limit cycle, if it exists, is hyperbolic. This implies that I has at most one zero in $]0, \mu[$ (counting its multiplicity).

Moreover, from [8, Theorem 1] it follows that system (23) has a crossing period annulus if and only if $\xi_0 = \xi_\infty = 0$. This implies that I is identically zero in this case.

Notice that the coefficient β from [8, Theorem 1] is zero and, if $\xi_0 = 0$, then

$$\text{sign}\left(\frac{a_{11}^+}{\sqrt{b^+ - a_{21}^+}}\right) = -\text{sign}(t^-) \text{ (recall that } b^+ > a_{21}^+\text{). The condition (H) from [8,}$$

Theorem 1] holds because $a_L = 1 > 0$, $a_R = -\sqrt{b^+ - a_{21}^+} < 0$ and $a_{12}^L a_{12}^R = (-1)(-1) = 1 > 0$ (the notation $a_L, a_R, a_{12}^L, a_{12}^R$ comes from [8]). These conditions can be easily checked after applying $(x, y) \to (y, x)$ to (23).   □

Remark 3 If the condition "$\xi_0 \neq 0$ or $\xi_\infty \neq 0$" of Theorem 3.1 is satisfied, then $\text{Cycl}(\cup_{x \in J} \Gamma_x) \leq 2$. This follows directly from Statement 2 of Theorems 2.2 and 3.1. Since the slow divergence integral I can have a simple zero in $]0, \mu[$ (see Theorems 4.3, 4.5, 4.7 and 4.9 in Sect. 4), a direct consequence of Statement 3 of Theorem 2.2 is that there exists a regularized PWL system (10) with 2 hyperbolic limit cycles.

Remark 4 We point out that limit cycles of (10) near so-called boundary graphics Γ_0 (the origin $(x, y) = (0, 0)$) and Γ_b cannot be studied using Theorem 3.1 and Theorem 2.2. As shown in the following section, the graphics Γ_b can contain (1) the zero x^* of the sliding vector-field X^{sl} as its corner point (in this case $\mu = x^*$ if $x^* > 0$ or $\mu = \Pi^{-1}(x^*)$ if $x^* < 0$), see e.g. Figure 4b, d in Sect. 4, (2) a hyperbolic saddle located away from the line $y = 0$, see Fig. 4a, c, e, (3) both the corner point x^* and the hyperbolic saddle away from $y = 0$, etc. This—along with the description of canard cycles in the half-plane with a visible fold—are topics of further study.

In this paper we do not treat periodic orbits of (10) when $I \equiv 0$. We leave this to future work. We expect that the analysis of such a case will depend upon the regularization function.

4 Case-by-Case Study of the Cyclicity of Canard Cycles

Theorem 3.1 in Sect. 3 provides an upper bound for the number of sliding limit cycles of system (10) (see Remark 3). In this section, we assume that $\xi_0 \neq 0$ or $\xi_\infty \neq 0$, with ξ_0, ξ_∞ defined in (22), and give detailed cyclicity results for (10), working with different phase portraits of Z^- (see Sect. 2.4). We distinguish between the saddle case (Theorem 4.3 in Sect. 4.2 and Remark 7), the node case (Theorems 4.5 and 4.7 in Sect. 4.3), the focus case (Theorem 4.9 in Sect. 4.4), the center case (Statement 2 of Theorem 4.1 and Appendix A) and the case without singularities (Statement 1 of Theorem 4.1 and Appendix B). We find that the slow divergence integral can have a zero in the hyperbolic cases (saddle, node and focus), but not in the remaining cases (center and the case without singularities). We provide sufficient and necessary

conditions for zeros of the slow divergence integral as well as information on boundary graphics (that will be relevant in future work).

Remark 5 It is not difficult to see that our sufficient conditions for a zero of the slow divergence integral are compatible with [8, corollary 2] [upon using the connection between zeros of the slow divergence integral and crossing cycles of the sewing system (23)]. Moreover, the part $I \neq 0$ of items 6–9 of Theorem 4.3, items 8–9 of Theorem 4.5, items 6–7 of Theorem 4.7, items 4–5 of Theorem 4.9, and of the center case follows from [10, Proposition 5]. Indeed, if system (23) has a crossing periodic orbit, then the traces must have opposite signs, that is, sign $\left(a_{11}^{+}\right) = -\text{sign}(t^{-})$.

Theorem 2.2 plays an important role in proving the above mentioned theorems. Let us denote by $\tilde{I}(x)$ the integral in (15). Using (21) it follows that

$$\tilde{I}'(x) = x(x - \Pi(x))\frac{a_{11}^{+}d^{-}x\Pi(x) + d^{-}(b^{+} - a_{21}^{+})(x + \Pi(x)) + \sqrt{b^{+} - a_{21}^{+}}\xi_0}{(1 + a_{21}^{+})X^{sl}(x)X^{sl}(\Pi(x))V(x)},$$
(24)

for all $x \in [0, \mu[$. From (24), $\Pi(x) < 0$ for $x > 0$ and the definition of the domain of Π and I it follows that

$$\tilde{I}'(x) = \Psi(x)\Delta(x),$$
(25)

where $\Psi(x) > 0$ for all $x \in]0, \mu[$ and

$$\Delta(x) = a_{11}^{+}d^{-}x\Pi(x) + d^{-}(b^{+} - a_{21}^{+})(x + \Pi(x)) + \sqrt{b^{+} - a_{21}^{+}}\xi_0.$$

Using (25) it is clear that $x = x_0 \in]0, \mu[$ is a zero of multiplicity l of $\tilde{I}'$ if and only if $x = x_0 \in]0, \mu[$ is a zero of multiplicity l of Δ.

We may assume that $t^{-} \geq 0$. Indeed, system (8) is invariant under the symmetry $(x, a_{11}^{+}, a_{22}^{+}, t^{-}, t) \rightarrow (-x, -a_{11}^{+}, -a_{22}^{+}, -t^{-}, -t)$, and, if we denote by $\Pi_{d^{-},t^{-}}$ (resp. $I_{d^{-},t^{-},b^{+},a_{11}^{+},a_{21}^{+}}$) the Poincaré half-map Π (resp. the slow divergence integral I) of (8), then using (15) we get

$$I_{d^{-},t^{-},b^{+},a_{11}^{+},a_{21}^{+}}(x) = -I_{d^{-},-t^{-},b^{+},-a_{11}^{+},a_{21}^{+}}(-\Pi_{d^{-},t^{-}}(x)).$$

$I_{d^{-},-t^{-},b^{+},-a_{11}^{+},a_{21}^{+}}$ is the slow divergence integral of (8) where $a_{11}^{+}, a_{22}^{+}, t^{-}$ are replaced with $-a_{11}^{+}, -a_{22}^{+}, -t^{-}$. Since $\Pi'_{d^{-},t^{-}} < 0$, the above formula implies that $x > 0$ is a zero of $I_{d^{-},t^{-},b^{+},a_{11}^{+},a_{21}^{+}}$ if and only if $-\Pi_{d^{-},t^{-}}(x) > 0$ is a zero of $I_{d^{-},-t^{-},b^{+},-a_{11}^{+},a_{21}^{+}}$ (with the same multiplicity). We conclude that the case $t^{-} < 0$ follows from the case $t^{-} > 0$.

First we prove the following theorem.

Theorem 4.1 *Consider the slow divergence integral $I(x)$, with $x \in [0, \mu[$, defined in* (15). *The following statements are true.*

1. *Suppose that $d^- = 0$ and $\xi_0 \neq 0$. Then the interval $[0, \mu[$ is bounded and, if $\xi_0 < 0$ (resp. $\xi_0 > 0$), then $I < 0$ (resp. $I > 0$) on $]0, \mu[$. For any small $\theta > 0$, we have $\mathrm{Cycl}(\cup_{x \in [\theta, \mu-\theta]} \Gamma_x) = 1$. The limit cycle is attracting (resp. repelling) if it exists.*

2. *Suppose that $\xi_\infty \neq 0$ and $t^- = 0$. Then the interval $[0, \mu[$ is bounded and, if $a_{11}^+ > 0$ (resp. $a_{11}^+ < 0$), then $I < 0$ (resp. $I > 0$) on $]0, \mu[$. For any small $\theta > 0$, $\mathrm{Cycl}(\cup_{x \in [\theta, \mu-\theta]} \Gamma_x) = 1$ and the limit cycle is attracting (resp. repelling) if it exists.*

Proof *Statement 1.* Suppose that $d^- = 0$ and $\xi_0 \neq 0$. If $t^- = 0$, then $a_{11}^+ \neq 0$ and the sliding vector field X^{sl} has a simple zero at $x = x^*$ defined in (12). This and the fact that for $d^- = t^- = 0$ the domain and image of Π are respectively $[0, +\infty[$ and $]-\infty, 0]$ (Sect. 2.4) imply that the domain $[0, \mu[$ of I is bounded. If $t^- > 0$, then the domain of Π is $[0, \frac{1}{t^-}[$ (Sect. 2.4), and $[0, \mu[\subset [0, \frac{1}{t^-}[$ is bounded.

Since $d^- = 0$, we have

$$\Delta(x) = \sqrt{b^+ - a_{21}^+} \xi_0,$$

with Δ defined in (25). Now, if $\xi_0 < 0$ (resp. $\xi_0 > 0$), then $\tilde{I}'(x), \Delta(x) < 0$ (resp. $\tilde{I}'(x), \Delta(x) > 0$) for all $x \in]0, \mu[$. Since $\tilde{I}(0) = 0$, we have that $\tilde{I}$ and I are negative (resp. positive) on $]0, \mu[$. The rest of the statement follows directly from Statement 1 of Theorem 2.2.

Statement 2. Suppose that $\xi_\infty \neq 0$ and $t^- = 0$. If $d^- < 0$, then $[0, \mu[$ is bounded because the domain of Π is bounded (see the saddle case in Sect. 2.4). If $d^- > 0$, then the domain and image of Π are respectively $[0, +\infty[$ and $]-\infty, 0]$ (see the center case in Sect. 2.4). Since x^* is well-defined ($a_{11}^+ \neq 0$), this implies that $[0, \mu[$ is bounded.

Since $t^- = 0$, we have $\Pi(x) = -x$ and

$$\Delta(x) = -a_{11}^+ V(x).$$

Notice that $V(x) = d^- x^2 + 1$ when $t^- = 0$. The function V is positive on the domain of Π. If $a_{11}^+ > 0$ (resp. $a_{11}^+ < 0$), then $\tilde{I}'(x) < 0$ (resp. $\tilde{I}'(x) > 0$) for all $x \in]0, \mu[$. The rest of the proof is now analogous to the proof in Statement 1. $\square$

For more details about the domain $[0, \mu[$ of I in Theorem 4.1 see Appendices A and B.

It remains to study the case where $d^- \neq 0$ and $t^- > 0$ (Sects. 4.1–4.4). We have Theorem 4.3 in Sect. 4.2 (the saddle case), Theorems 4.5 and 4.7 in Sect. 4.3 (the node case) and Theorem 4.9 in Sect. 4.4 (the focus case).

The main idea in the proof of the above mentioned theorems is to study mutual positions of the curve $y = \Pi(x)$ and the curve $\overline{\Delta}(x, y) = 0$ where

$$\overline{\Delta}(x, y) = a_{11}^+ d^- xy + d^- (b^+ - a_{21}^+)(x + y) + \sqrt{b^+ - a_{21}^+} \xi_0. \tag{26}$$

We will see that, for $d^- \neq 0$ and $t^- > 0$, there is at most 1 intersection (multiplicity counted) between the curve $y = \Pi(x)$ and the curve $\overline{\Delta}(x, y) = 0$ in the fourth quadrant

with $x \in]0, \mu[$. Then this implies that $\Delta(x) = \overline{\Delta}(x, \Pi(x))$ (or, equivalently, $\tilde{I}'$) has at most 1 zero counting multiplicity in $]0, \mu[$. Using Rolle's theorem and $\tilde{I}(0) = 0$, we conclude that $\tilde{I}$ (or I) has at most 1 zero counting multiplicity in $]0, \mu[$ (see also Theorem 3.1).

Remark 6 The function $\overline{\Delta}$ corresponds to the function F in [10, Eq. (23)]. This relates to a connection between the sign of $\tilde{I}'(x)$ (which determines the stability of the sliding (canard) cycles for $0 < \epsilon \ll 1$) and the stability of the corresponding crossing cycles of the related sewing system (23). It is therefore also our expectation that the case-dependent results in the present section, can be obtained by working on (23). In fact, [45, Theorem 2] applied to (23) implies, under assumptions of item 5 of Theorem 4.9, that I has at most one zero. From [53, Theorem 1.1] it follows that (23) has no limit cycles (resp. at most one limit cycle) if $a_{11}^+ t^- \geq 0$ (resp. $a_{11}^+ t^- < 0$). We will not pursue the connection to (23) further in the present manuscript.

In Sect. 4.1 we classify the curves defined by the equation $\overline{\Delta}(x, y) = 0$ and find contact points between these curves and the orbits of system (34) defined in Sect. 4.1.

4.1 Properties of the Curves Defined by $\overline{\Delta} = 0$

Consider the function $\overline{\Delta}$ defined in (26). In further details, notice first that

$$\overline{\Delta}(x, y) = \overline{\Delta}(y, x), \tag{27}$$

$$\nabla\overline{\Delta}(x, y) = \begin{bmatrix} (1 + a_{21}^+)d^- X^{sl}(y) \\ (1 + a_{21}^+)d^- X^{sl}(x) \end{bmatrix}, \tag{28}$$

$$\overline{\Delta}(x, x^*) = -a_{11}^+ V(x^*). \tag{29}$$

Then, for $d^- \neq 0$ and $t^- > 0$, we distinguish between the following 3 cases.

1. If $a_{11}^+ d^- \neq 0$, $t^- > 0$ and $V(x^*) = 0$, with x^* defined in (12), then by (27) and (29)

$$\overline{\Delta}(x, y) = a_{11}^+ d^- (x - x^*)(y - x^*), \tag{30}$$

and $\overline{\Delta}(x, y) = 0$ therefore represents the union of two lines $x = x^*$ and $y = x^*$. In this case we will see that $y = \Pi(x)$ and $\overline{\Delta}(x, y) = 0$ have no intersection points. For further details, see Sects. 4.2 and 4.3.

2. If $a_{11}^+ d^- \neq 0$, $t^- > 0$ and $V(x^*) \neq 0$, then $\overline{\Delta}(x, y) = 0$ represents a hyperbola

$$y = hp(x) := \frac{-\sqrt{b^+ - a_{21}^+ \xi_0} - d^-(b^+ - a_{21}^+)x}{d^-(1 + a_{21}^+)X^{sl}(x)}. \tag{31}$$

It follows from (27) that the function hp is an involution. The graph of $y = hp(x)$ has a vertical asymptote $x = x^*$ and a horizontal asymptote $y = x^*$, and

$$hp(0) = \frac{t^- x^* - 1}{d^- x^*}, \quad hp'(x) = -\frac{(a_{11}^+)^2 V(x^*)}{d^-(1 + a_{21}^+)^2 X^{sl}(x)^2}. \tag{32}$$

In this case we will prove that $y = \Pi(x)$ and $\overline{\Delta}(x, y) = 0$ have at most 1 intersection counting multiplicity in the fourth quadrant with $x \in]0, \mu[$. Moreover, we show the existence of a transversal intersection for some parameter values satisfying the above condition. See Sects. 4.2–4.4.

3. If $a_{11}^+ = 0$, $d^- \neq 0$ and $t^- > 0$, then $\overline{\Delta}(x, y) = 0$ represents a line

$$y = \frac{t^-}{d^-} - x. \tag{33}$$

In this case we prove that $y = \Pi(x)$ and $\overline{\Delta}(x, y) = 0$ have no intersection points. See Sects. 4.2–4.4.

It can be easily seen that in cases 1–3 we have $\overline{\Delta}(x_L, x_R) = \overline{\Delta}(x_R, x_L) = 0$ where x_L and x_R are defined in (20).

Lemma 4.2 *Suppose that $d^- \neq 0$ and $t^- > 0$. Consider the function $\Delta(x)$ defined in (25), with $x \in]0, \mu[$, and $\overline{\Delta}$ defined in (26). The following statements are true.*

1. *Suppose that $d^- < 0$. If the curve $\overline{\Delta}(x, y) = 0$ lies above (resp. below) the curve $y = \Pi(x)$ for all x kept in an interval $J \subset]0, \mu[$, then $\Delta(x), \tilde{I}'(x) > 0$ (resp. $\Delta(x), \tilde{I}'(x) < 0$) for all $x \in J$.*
2. *Suppose that $d^- > 0$. If the curve $\overline{\Delta}(x, y) = 0$ lies above (resp. below) the curve $y = \Pi(x)$ for all x kept in an interval $J \subset]0, \mu[$, then $\Delta(x), \tilde{I}'(x) < 0$ (resp. $\Delta(x), \tilde{I}'(x) > 0$) for all $x \in J$.*

Proof We will prove Statement 1. Statement 2 can be proved in the same fashion as Statement 1.

Let $d^- < 0$. Suppose first that $a_{11}^+ \neq 0$ and $V(x^*) = 0$. Then $\overline{\Delta}$ is given in (30). If the curve $\overline{\Delta}(x, y) = 0$ (that is, $y = x^*$) lies above the curve $y = \Pi(x)$ with $x \in J \subset]0, \mu[$, then $x^* > \Pi(x)$ for all $x \in J$. Using (30) we get

$$\Delta(x) = \overline{\Delta}(x, \Pi(x)) = a_{11}^+ d^- (x - x^*)(\Pi(x) - x^*) > 0, \ \forall x \in J.$$

We used $d^- < 0$, $x^* > \Pi(x)$ for all $x \in J$ and $a_{11}^+(x - x^*) > 0$ for all $x \in J$. Let us prove that $a_{11}^+(x - x^*) > 0$ for all $x \in J$. If $a_{11}^+ > 0$, then (12) implies that $x^* < 0$. Since $x > 0$ for all $x \in J$, it follows that $a_{11}^+(x - x^*) > 0$ for all $x \in J$. If $a_{11}^+ < 0$, then $x^* > 0$. Using the definition of the domain $[0, \mu[$ of I (Sect. 3), it is clear that $\mu \leq x^*$. Thus, $x < x^*$ for all $x \in J$. This implies that $a_{11}^+(x - x^*) > 0$ for all $x \in J$. The case where the curve $\overline{\Delta}(x, y) = 0$ (that is, $y = x^*$) lies below the curve $y = \Pi(x)$ can be studied in a similar way. We get $\Delta(x) < 0$ for all $x \in J$.

Now, suppose that $a_{11}^+ \neq 0$ and $V(x^*) \neq 0$. If the curve $\overline{\Delta}(x, y) = 0$ lies above the curve $y = \Pi(x)$ with $x \in J$, then $hp(x) > \Pi(x)$ for all $x \in J$, with hp defined in (31). If we substitute (31) in $hp(x) > \Pi(x)$ and if we use $d^- < 0$, then we get $\Delta(x) > 0$ for all $x \in J$. The case where the curve $\overline{\Delta}(x, y) = 0$ lies below the curve $y = \Pi(x)$ can be studied in a similar way. We obtain $\Delta(x) < 0$ for all $x \in J$.

Finally, suppose that $a_{11}^+ = 0$. If the curve $\overline{\Delta}(x, y) = 0$ lies above the curve $y = \Pi(x)$ with $x \in J$, then $\frac{t^-}{d^-} - x > \Pi(x)$ for all $x \in J$. We use (33). Since $d^- < 0$, we have $\Delta(x) > 0$ for all $x \in J$. The case where the curve $\overline{\Delta}(x, y) = 0$ lies below the curve $y = \Pi(x)$ can be studied in a similar way. We have $\Delta(x) < 0$ for all $x \in J$.
□

Notice that $y = \Pi(x)$ is the $x \geq 0$-subset of the stable manifold of the hyperbolic saddle point $(x, y) = (0, 0)$ of the following polynomial system of degree 3

$$
\begin{aligned}
\dot{x} &= yV(x), \\
\dot{y} &= xV(y).
\end{aligned}
\tag{34}
$$

This can be easily seen from (21) (see also [6, Remark 16]). It is clear that system (34) is invariant under the symmetry $(x, y) \to (y, x)$. It is important (Sects. 4.2–4.4) to calculate the number of contact points between the orbits of system (34) and the curve $\overline{\Delta}(x, y) = 0$. The contact points are solutions of

$$
\begin{aligned}
\nabla\overline{\Delta}(x, y) \cdot (yV(x), xV(y)) &= 0, \\
\overline{\Delta}(x, y) &= 0.
\end{aligned}
\tag{35}
$$

Using (28) the first equation in (35) becomes

$$
(1 + a_{21}^+)d^- \left(xV(y)X^{sl}(x) + yV(x)X^{sl}(y) \right) = 0
\tag{36}
$$

Recall that $X^{sl}(x^*) = 0$ for $a_{11}^+ \neq 0$. Therefore if $a_{11}^+ d^- \neq 0$, $t^- > 0$ and $V(x^*) = 0$, then (36) implies that all points on the lines $x = x^*$ and $y = x^*$ are the contact points. On the other hand, if $a_{11}^+ d^- \neq 0$, $t^- > 0$ and $V(x^*) \neq 0$ and if we substitute (31) in (36), we get the following equation for contact points

$$
V(x) \left(-\sqrt{b^+ - a_{21}^+ \xi_0} + a_{11}^+ d^- x^2 \right) = 0.
\tag{37}
$$

Using (37) the contact points are: $(x, y) = (x_L, x_R)$, $(x, y) = (x_R, x_L)$ (if $(t^-)^2 - 4d^- \geq 0$), and $(x, y) = (x_C, -x_C)$ and $(x, y) = (-x_C, x_C)$ where

$$
x_C = \sqrt{\frac{t^- x^* - 1}{d^-}},
\tag{38}
$$

if $\frac{t^- x^* - 1}{d^-} \geq 0$. Let us recall that x_L, x_R are defined in (20) and x^* is defined in (12).

When $d^- \neq 0$, $t^- > 0$ and $a_{11}^+ = 0$, then we substitute (33) in (36) and get the following equation for contact points:

$$V(x) = 0. \tag{39}$$

4.2 The Saddle Case

In this section we suppose that $d^- < 0$. Then Z^- has a hyperbolic saddle at $(x, y) = (\frac{t^-}{d^-}, \frac{1}{d^-})$ with eigenvalues $\varkappa_- < 0$ and $\varkappa_+ > 0$ given in (17). From (18) it follows that the stable manifold of the hyperbolic saddle is given by $x = \varkappa_+ y + x_R$ and the unstable manifold is given by $x = \varkappa_- y + x_L$ where $x_L < 0$ and $x_R > 0$ are defined in (20). It is clear that the stable (resp. unstable) manifold intersects the x-axis at $x = x_R$ (resp. $x = x_L$). We refer to Fig. 4.

From Fig. 4 it follows that the domain and image of Π are respectively $[0, x_R[$ and $]x_L, 0]$ (see also [6]). The domain of the slow divergence integral I (or $\tilde{I}$) depends on the location of the singularity $x = x^*$ of the sliding vector field. We distinguish between 5 cases.

(a) If $a_{11}^+ < 0$ (hence $x^* > 0$) and $x_R \leq x^*$, then the domain of I is $[0, x_R[$ and we consider the canard cycle Γ_x for all $x \in]0, x_R[$ (see Fig. 4a).
(b) If $a_{11}^+ < 0$ and $x^* < x_R$, then the domain of I is $[0, x^*[$ and we consider the canard cycle Γ_x for all $x \in]0, x^*[$ (see Fig. 4b).
(c) If $a_{11}^+ = 0$, then we have the same domain of I as in the case (a) (see Fig. 4c).
(d) If $a_{11}^+ > 0$ (hence $x^* < 0$) and $x_L < x^*$, then the domain of I is $[0, \Pi^{-1}(x^*)[$ and we consider the canard cycle Γ_x for all $x \in]0, \Pi^{-1}(x^*)[$ (see Fig. 4d).
(e) If $a_{11}^+ > 0$ (hence $x^* < 0$) and $x^* \leq x_L$, then we deal with the same domain of I as in the case (a) (see Fig. 4e).

Besides the hyperbolic saddle at the origin, the system (34) has hyperbolic and attracting nodes at $(x, y) = (x_R, x_R)$ and $(x, y) = (x_L, x_L)$, and hyperbolic and repelling nodes at $(x, y) = (x_R, x_L)$ and $(x, y) = (x_L, x_R)$. Notice that the lines $x = x_R$, $x = x_L$, $y = x_R$ and $y = x_L$ are invariant (Fig. 5). Let us focus on the singularity $(x, y) = (x_R, x_L)$ in the fourth quadrant. Since $t^- > 0$, it is easy to see that the straight-line solution corresponding to the weaker eigenvalue of $(x, y) = (x_R, x_L)$ is $x = x_R$, and the regular orbit of (34) given by $y = \Pi(x)$ tends to $(x, y) = (x_R, x_L)$ tangentially to the straight-line $x = x_R$ (in backward time).

A detailed statement of Theorem 4.3 below covers all possible mutual positions of the curve $y = \Pi(x)$ and the curve $\overline{\Delta}(x, y) = 0$ (see Fig. 5).

Theorem 4.3 *Suppose that $d^- < 0$ and $t^- > 0$. Then $x_R < \frac{1}{t^-}$ and the following statements are true.*

1. *($a_{11}^+ < 0$) If $\frac{1}{t^-} < x^*$ (Fig. 5a), then we have $I < 0$ on $]0, x_R[$ and, for any small $\theta > 0$, $\mathrm{Cycl}(\cup_{x \in [\theta, x_R - \theta]}\Gamma_x) = 1$. The limit cycle is attracting.*
2. *($a_{11}^+ < 0$) If $x^* = \frac{1}{t^-}$ (Fig. 5b), then we have $I < 0$ on $]0, x_R[$ and, for any small $\theta > 0$, $\mathrm{Cycl}(\cup_{x \in [\theta, x_R - \theta]}\Gamma_x) = 1$. The limit cycle is attracting.*
3. *($a_{11}^+ < 0$) If $x_R < x^* < \frac{1}{t^-}$ (Fig. 5c), then the function I has at most 1 zero (counting multiplicity) on $]0, x_R[$ and, for any small $\theta > 0$, $\mathrm{Cycl}(\cup_{x \in [\theta, x_R - \theta]}\Gamma_x) \leq 2$.*
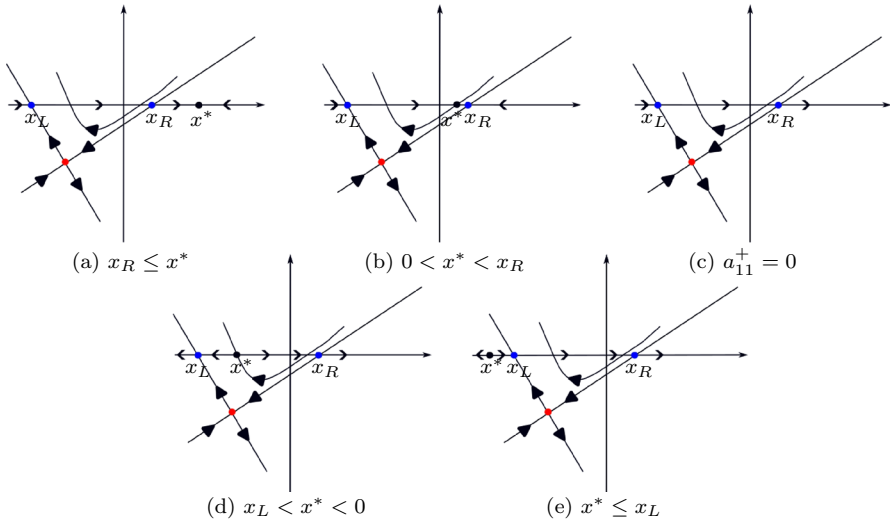
(a) $x_R \leq x^*$ (b) $0 < x^* < x_R$ (c) $a_{11}^+ = 0$

(d) $x_L < x^* < 0$ (e) $x^* \leq x_L$

Fig. 4 Phase portraits of Z^-, with $d^- < 0$ and $t^- > 0$, defined in (8) and the direction of the sliding vector field (11) along $y = 0$. Z^- has a hyperbolic saddle. We do not draw the corresponding phase portraits of Z^+

There exists x^* *(sufficiently close to* $\frac{1}{t^-}$*) such that I has a simple zero in* $]0, x_R[$
and then, for any sufficiently small $\theta > 0$, Cycl$(\cup_{x \in [\theta, x_R - \theta]} \Gamma_x) = 2$.

4. *($a_{11}^+ < 0$) If $x^* = x_R$ (Fig. 5d), then $I > 0$ on* $]0, x_R[$ *and, for any small $\theta > 0$, Cycl$(\cup_{x \in [\theta, x_R - \theta]} \Gamma_x) = 1$ (the limit cycle is repelling).*

5. *($a_{11}^+ < 0$) If $0 < x^* < x_R$ (Fig. 5e), then we have $I > 0$ on* $]0, x^*[$ *and, for any small $\theta > 0$, Cycl$(\cup_{x \in [\theta, x^* - \theta]} \Gamma_x) = 1$ (the limit cycle is repelling).*

6. *($a_{11}^+ > 0$) If $x_L < x^* < 0$ (Fig. 5f), then we have $I < 0$ on* $]0, \Pi^{-1}(x^*)[$ *and, for any small $\theta > 0$, Cycl$(\cup_{x \in [\theta, \Pi^{-1}(x^*) - \theta]} \Gamma_x) = 1$ (the limit cycle is attracting).*

7. *($a_{11}^+ > 0$) If $x^* = x_L$ (Fig. 5g), we have $I < 0$ on* $]0, x_R[$ *and, for any small $\theta > 0$, Cycl$(\cup_{x \in [\theta, x_R - \theta]} \Gamma_x) = 1$ (the limit cycle is attracting).*

8. *($a_{11}^+ > 0$) If $x^* < x_L$ (Fig. 5h), then we have $I < 0$ on* $]0, x_R[$ *and, for any small $\theta > 0$, Cycl$(\cup_{x \in [\theta, x_R - \theta]} \Gamma_x) = 1$ (the limit cycle is attracting).*

9. *If $a_{11}^+ = 0$ (Fig. 5i), we have $I < 0$ on* $]0, x_R[$ *and, for any small $\theta > 0$, Cycl$(\cup_{x \in [\theta, x_R - \theta]} \Gamma_x) = 1$ (the limit cycle is attracting).*

Proof Suppose that $d^- < 0$ and $t^- > 0$. Using (20) we know that

$$x_L = \frac{2}{t^- - \sqrt{(t^-)^2 - 4d^-}} < 0, \quad x_R = \frac{2}{t^- + \sqrt{(t^-)^2 - 4d^-}} > 0,$$

$V(x_L) = V(x_R) = 0$ where $V(x) = d^- x^2 - t^- x + 1$. The graph of V is concave down because $d^- < 0$. Using the expression for x_R it can be easily seen that $x_R < \frac{1}{t^-}$. Notice that $x_C \geq 0$ in (38) is well-defined if $x^* \leq \frac{1}{t^-}$. We have
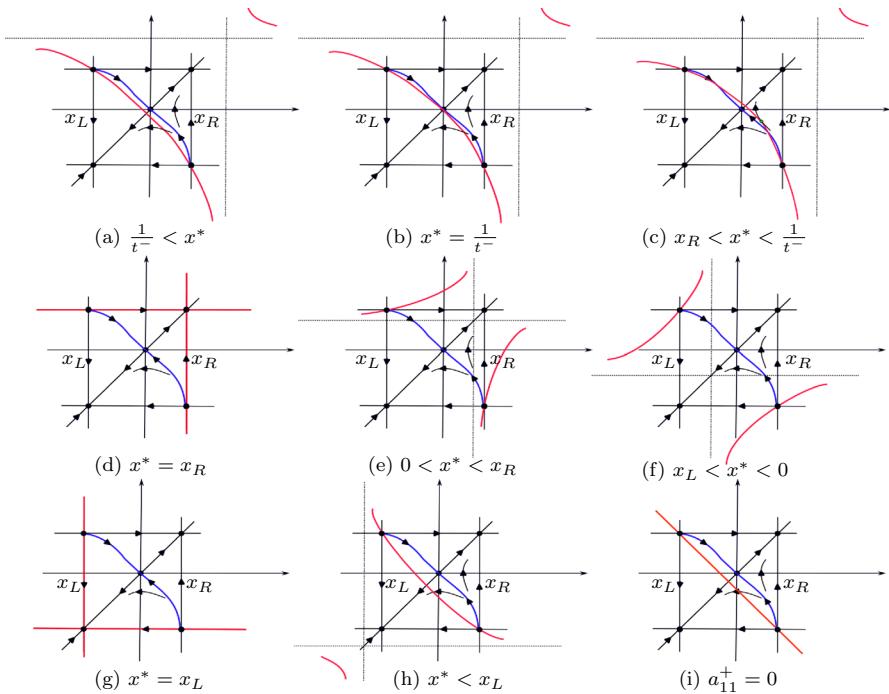
Fig. 5 The phase portrait of (34) for $d^- < 0$ and $t^- > 0$, with the curve $\overline{\Delta}(x, y) = 0$ (red). The part of the blue curve located in the fourth quadrant is the graph of Π. We draw the vertical and horizontal lines $x = x^*$ and $y = x^*$ using dashed lines. $(x, y) = (x_C, -x_C)$ and $(x, y) = (-x_C, x_C)$ are the intersection points between the red curve and $y = -x$. We indicate the contact point $(x, y) = (x_C, -x_C)$ when x_C is positive and contained in the domain of the slow divergence integral I (**c**) (Color figure online)

Lemma 4.4 *Suppose that* $d^- < 0$, $a_{11}^+ \neq 0$, $t^- > 0$ *and* $V(x^*) \neq 0$ *(i.e.* $x^* \neq x_L, x_R$). *Then the following statements are true.*

1. *If* $x^* = \frac{1}{t^-}$, *then* $x_C = 0$.
2. *If* $x_R < x^* < \frac{1}{t^-}$, *then* $0 < x_C < x_R$.
3. *If* $x_L < x^* < x_R$, *then* $x_R < x_C < -x_L$.
4. *If* $x^* < x_L$, *then* $-x_L < x_C < -x^*$.

Proof of Lemma 4.4 This follows from elementary calculus using the above expressions for $x_{L,R}$ and $x_C = \sqrt{\frac{t^- x^* - 1}{d^-}}$. $\qquad\square$

The expressions for $hp(0)$ and $hp'(x)$ are given in (32).

Proof of Statement 1 of Theorem 4.3. Suppose that $\frac{1}{t^-} < x^*$. Then $hp(0) < 0$. Since $x_R < \frac{1}{t^-}$, we have $x_R < x^*$ and $V(x^*) < 0$. This, together with (32), implies that $hp'(x) < 0$ for all $x \neq x^*$. The graph of hp is given in Fig. 5a (see the red curve). Since $\frac{1}{t^-} < x^*$, the contact points between the orbits of system (34) and $y = hp(x)$ are $(x, y) = (x_L, x_R)$ and $(x, y) = (x_R, x_L)$. See the paragraph after (37).

Since $x_R < x^*$, the domain of I is $[0, x_R[$ (see Fig. 4a). We show that $I < 0$ on $]0, x_R[$. Since $I(0) = 0$, it suffices to prove that $I' < 0$ (equivalently, $\tilde{I}' < 0$ or $\Delta < 0$)

on $]0, x_R[$ (see (25)). We prove that the graph of hp is located below the graph of Π for $x \in]0, x_R[$. Then Statement 1 of Lemma 4.2 will imply that $I' < 0$ on $]0, x_R[$.

Using $hp(0) < 0$ and the paragraph before Theorem 4.3, it is clear that the graph of hp lies below the graph of Π for $x > 0$ and $x \sim 0$ and for $x < x_R$ and $x \sim x_R$. If we assume that there exists an intersection point between the graph of hp and the graph of Π for $x \in]0, x_R[$, then there is a contact point between the orbits of system (34) and $y = hp(x)$ because (34) has a saddle at $(x, y) = (0, 0)$. The $x-$component of the contact point is contained in $]0, x_R[$. This is in direct contradiction with the fact that $(x, y) = (x_L, x_R)$ and $(x, y) = (x_R, x_L)$ are the only possible contact points. Thus, the graph of hp lies below the graph of Π for $x \in]0, x_R[$. From Statement 1 of Theorem 2.2 it follows that for any small $\theta > 0$, $\mathrm{Cycl}(\cup_{x \in [\theta, x_R - \theta]} \Gamma_x) = 1$ (the limit cycle is attracting because I is negative).

Statement 2. Suppose that $x^* = \frac{1}{t^-}$. Then (32) implies that $hp(0) = 0$. Since $x_R < \frac{1}{t^-} = x^*$, we have $hp'(x) < 0$ for all $x \neq x^*$ and the domain of I is $[0, x_R[$ (see the proof of Statement 1). The graph of hp is given in Fig. 5b (the red curve). From Lemma 4.4 (Statement 1) it follows that the contact points between the orbits of system (34) and $y = hp(x)$ are $(x, y) = (x_L, x_R)$, $(x, y) = (x_R, x_L)$ and $(x, y) = (0, 0)$.

We prove that the graph of hp lies below the graph of Π for $x \in]0, x_R[$. This will imply that $I < 0$ on $]0, x_R[$ (see the proof of Statement 1). Clearly, the graph of hp lies below the graph of Π for $x < x_R$ and $x \sim x_R$. If there is an intersection point between the graph of hp and the graph of Π for $x \in]0, x_R[$, then we have an extra contact point between the orbits of system (34) and $y = hp(x)$, with the $x-$component contained in $]0, x_R[$. This contact point is different from $(x, y) = (x_L, x_R)$, $(x, y) = (x_R, x_L)$ and $(x, y) = (0, 0)$. This gives a contradiction and implies that the graph of hp lies below the graph of Π for $x \in]0, x_R[$. The rest of the Statement follows directly from Statement 1 of Theorem 2.2.

Statement 3. Assume that $x_R < x^* < \frac{1}{t^-}$. From (32) it follows that $hp(0) > 0$. Since $x_R < x^*$, we have $hp'(x) < 0$ for all $x \neq x^*$ and the domain of I is $[0, x_R[$ (see again the proof of Statement 1). The graph of hp is given in Fig. 5c. Lemma 4.4 (Statement 2) implies that the contact points between the orbits of system (34) and $y = hp(x)$ are $(x, y) = (x_L, x_R)$, $(x, y) = (x_R, x_L)$, $(x, y) = (x_C, -x_C)$ and $(x, y) = (-x_C, x_C)$, with $0 < x_C < x_R$.

First we prove that there is precisely 1 intersection (counting multiplicity) between the graph of hp and the graph of Π for $x \in]0, x_R[$. This will imply that I' has 1 zero (counting multiplicity) on $]0, x_R[$. Using Rolle's theorem and $I(0) = 0$ we find at most 1 zero (counting multiplicity) of I on $]0, x_R[$. Then, from Statement 2 of Theorem 2.2 it follows that for any small $\theta > 0$ the set $\cup_{x \in [\theta, x_R - \theta]} \Gamma_x$ can produce at most 2 limit cycles. The graph of hp lies below the graph of Π for $x < x_R$ and $x \sim x_R$ (see the proof of Statement 1) and, since $hp(0) > 0$, the graph of hp lies above the graph of Π for $x > 0$ and $x \sim 0$. Thus, there exists at least 1 intersection between the graph of hp and the graph of Π for $x \in]0, x_R[$ (The Intermediate-Value Theorem). If we assume that we have at least 2 intersections (counting multiplicity), then, besides $(x, y) = (x_C, -x_C)$, we find at least 1 extra contact point with the $x-$component contained in $]0, x_R[$. This gives a contradiction. Thus, there exists precisely 1 intersection (counting multiplicity).

Let us prove that I has a (simple) zero in $]0, x_R[$ if $x_R < x^* < \frac{1}{t^-}$ and if x^* is close enough to $\frac{1}{t^-}$. Statement 2 implies the existence of $x_0 \in]0, x_R[$ such that $I(x_0) < 0$ for each $x^* < \frac{1}{t^-}$ and $x^* \sim \frac{1}{t^-}$ (I is continuous). On the other hand, we know that the graph of hp lies above the graph of Π for $x > 0$ and $x \sim 0$. Then Statement 1 of Lemma 4.2 implies that $I'(x) > 0$ for all $x > 0$ and $x \sim 0$. Since $I(0) = 0$, we have $I(x) > 0$ for all $x > 0$ and $x \sim 0$. From The Intermediate-Value Theorem it follows now that I has a zero in $]0, x_R[$ when x^* is close enough to $\frac{1}{t^-}$. Then Statement 3 of Theorem 2.2 implies that for any sufficiently small $\theta > 0$, $\text{Cycl}(\cup_{x \in [\theta, x_R - \theta]}\Gamma_x) = 2$.

Statement 4. Suppose that $x^* = x_R$. The domain of I is $[0, x_R[$ (see the proof of Statement 1). Since $a_{11}^+ d^- \neq 0$ and $V(x^*) = 0$, points on the lines $x = x_R$ and $y = x_R$ are solutions of $\overline{\Delta} = 0$ (see Fig. 5d). Since the line $y = x_R$ lies above the graph of Π for $x \in]0, x_R[$, Statement 1 of Lemma 4.2 implies that $\tilde{I}'(x) > 0$ (i.e., $I'(x) > 0$) for all $x \in]0, x_R[$. Thus, $I > 0$ on $]0, x_R[$. The rest of Statement 4 follows from Statement 1 of Theorem 2.2.

Statement 5. Suppose that $0 < x^* < x_R$. Then (32) and $V(x^*) > 0$ imply that $hp(0) > 0$ and $hp'(x) > 0$ for all $x \neq x^*$. The graph of hp is given in Fig. 5e.

Since $0 < x^* < x_R$, the domain of I is $[0, x^*[$ (see Fig. 4b). Clearly, the graph of hp lies above the graph of Π for $x \in]0, x^*[$ and Statement 1 of Lemma 4.2 implies that $I'(x) > 0$ for all $x \in]0, x^*[$. Thus, $I > 0$ on $]0, x^*[$. The rest of Statement 5 follows from Statement 1 of Theorem 2.2.

Statement 6. Suppose that $x_L < x^* < 0$. From (32) and $V(x^*) > 0$ it follows that $hp(0) < 0$ and $hp'(x) > 0$ for all $x \neq x^*$. The graph of hp is given in Fig. 5f.

Since $x_L < x^* < 0$, the domain of I is $[0, \Pi^{-1}(x^*)[$ (Fig. 4d). It is clear that the graph of hp lies below the graph of Π for $x \in]0, \Pi^{-1}(x^*)[$ and $I'(x) < 0$ for all $x \in]0, \Pi^{-1}(x^*)[$ (see Statement 1 of Lemma 4.2). Thus, $I < 0$ on $]0, \Pi^{-1}(x^*)[$. The rest of Statement 6 follows from Statement 1 of Theorem 2.2.

Statement 7. The proof of Statement 7 is similar to the proof of Statement 4. Since $x^* = x_L$, the domain of I is $[0, x_R[$ (Fig. 4e).

Statement 8. Suppose that $x^* < x_L$. From (32) and $V(x^*) < 0$ it follows that $hp(0) < 0$ and $hp'(x) < 0$ for all $x \neq x^*$. The graph of hp is given in Fig. 5h. We use Statement 4 of Lemma 4.4 and see that the contact points are $(x, y) = (x_L, x_R)$, $(x, y) = (x_R, x_L)$, $(x, y) = (x_C, -x_C)$ and $(x, y) = (-x_C, x_C)$, with $-x_L < x_C < -x^*$.

Since $x^* < x_L$, the domain of I is $[0, x_R[$ (Fig. 4e). We can prove that the graph of hp lies below the graph of Π for $x \in]0, x_R[$ (see the proof of Statement 1). Notice that the $x-$coordinate of the above contact points is not contained in $]0, x_R[$.

Statement 9. Suppose that $a_{11}^+ = 0$. Let us recall that $d^- < 0$ and $t^- > 0$. The solutions of $\overline{\Delta} = 0$ are given by (33) (see the red line in Fig. 5i). From (39) it follows that the contact points between the orbits of system (34) and the line given in (33) are $(x, y) = (x_L, x_R)$ and $(x, y) = (x_R, x_L)$.

The domain of I is $[0, x_R[$ (Fig. 4c). We can show that the line (33) lies below the graph of Π for $x \in]0, x_R[$ (see the proof of Statement 1). □

4.3 The Node Case

4.3.1 Distinct Eigenvalues

In this section we assume that $d^- > 0$, $t^- > 0$ and $(t^-)^2 - 4d^- > 0$. System Z^- has a repelling node at $(x, y) = (\frac{t^-}{d^-}, \frac{1}{d^-})$ with eigenvalues $0 < \varkappa_- < \varkappa_+$ where $\varkappa_\pm$ are given in (17). The straight-line solution corresponding to the eigenvalue $\varkappa_-$ (resp. $\varkappa_+$) is given by $x = \varkappa_+ y + x_L$ (resp. $x = \varkappa_- y + x_R$) where $0 < x_L < x_R$ are defined in (20). We refer to Lemma 2.3 and Fig. 6.

Using Fig. 6 we see that the domain and image of Π are respectively $[0, x_L[$ and $]-\infty, 0]$ (see also [6]). The domain of the slow divergence integral I (or $\tilde{I}$) depends on x^*. We distinguish between 4 cases.

(a) If $a_{11}^+ < 0$ (hence $x^* > 0$) and $x_L \le x^*$, then the domain of I is $[0, x_L[$ and we consider the canard cycle Γ_x for all $x \in]0, x_L[$ (see Fig. 6a).
(b) If $a_{11}^+ < 0$ and $x^* < x_L$, then the domain of I is $[0, x^*[$ and we consider the canard cycle Γ_x for all $x \in]0, x^*[$ (see Fig. 6b).
(c) If $a_{11}^+ = 0$, then we have the same domain of I as in the case (a) (see Fig. 6c).
(d) If $a_{11}^+ > 0$ (hence $x^* < 0$), then the domain of I is $[0, \Pi^{-1}(x^*)[$ and we consider the canard cycle Γ_x for all $x \in]0, \Pi^{-1}(x^*)[$ (see Fig. 6d).

Apart from the hyperbolic saddle at the origin, system (34) has a hyperbolic and attracting node at $(x, y) = (x_L, x_L)$, a hyperbolic and repelling node at $(x, y) = (x_R, x_R)$, and hyperbolic saddles at $(x, y) = (x_R, x_L)$ and $(x, y) = (x_L, x_R)$ (Fig. 7). Notice that the invariant line $x = x_L$ is the vertical asymptote for the graph of the Poincaré half-map Π.

Theorem 4.5 *Suppose that $d^- > 0$, $t^- > 0$ and $(t^-)^2 - 4d^- > 0$. Then $\frac{1}{t^-} < x_L$ and the following statements are true.*

1. *($a_{11}^+ < 0$) If $x_R < x^*$ (Fig. 7a), we have $I < 0$ on $]0, x_L[$ and, for any small $\theta > 0$, $\mathrm{Cycl}(\cup_{x \in [\theta, x_L - \theta]} \Gamma_x) = 1$ (the limit cycle is attracting).*
2. *($a_{11}^+ < 0$) If $x^* = x_R$ (Fig. 7b), then we have $I < 0$ on $]0, x_L[$ and, for any small $\theta > 0$, $\mathrm{Cycl}(\cup_{x \in [\theta, x_L - \theta]} \Gamma_x) = 1$ (the limit cycle is attracting).*
3. *($a_{11}^+ < 0$) If $x_L < x^* < x_R$ (Fig. 7c), then we have $I < 0$ on $]0, x_L[$ and, for any small $\theta > 0$, $\mathrm{Cycl}(\cup_{x \in [\theta, x_L - \theta]} \Gamma_x) = 1$. The limit cycle is attracting.*

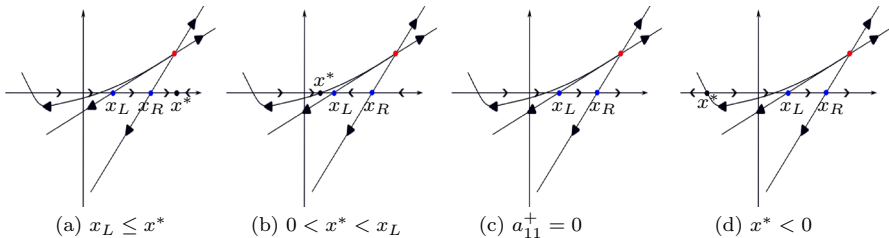(a) $x_L \le x^*$　　　　(b) $0 < x^* < x_L$　　　　(c) $a_{11}^+ = 0$　　　　(d) $x^* < 0$

Fig. 6 Phase portraits of Z^- defined in (8) and the direction of the sliding vector field (11) along $y = 0$, for $d^- > 0$, $t^- > 0$ and $(t^-)^2 - 4d^- > 0$. Z^- has a repelling node with distinct eigenvalues. We do not draw the corresponding phase portraits of Z^+
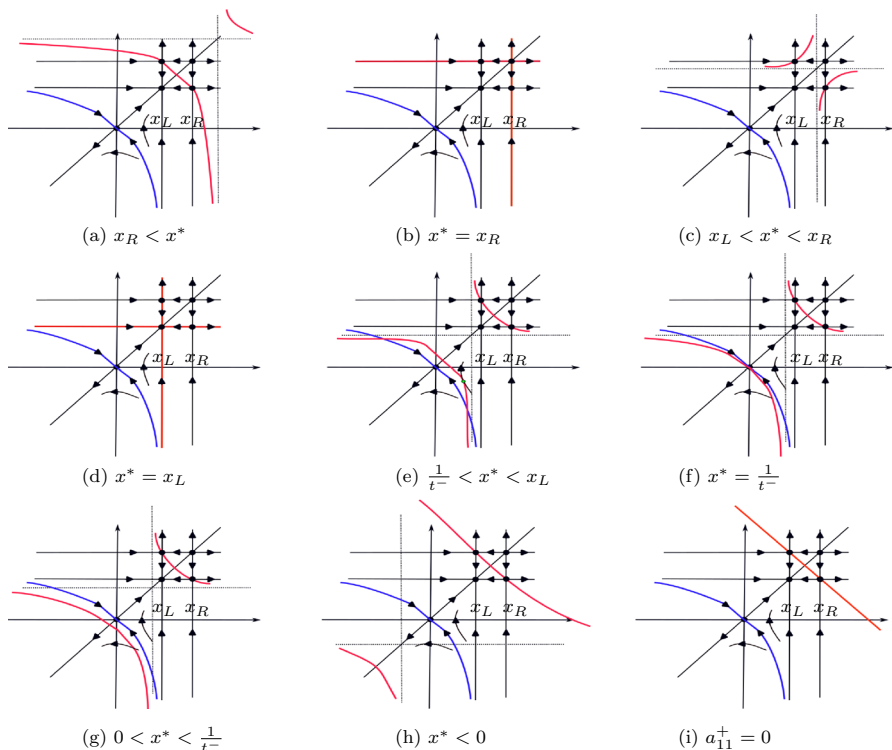
Fig. 7 The phase portrait of (34) for $d^- > 0$, $t^- > 0$ and $(t^-)^2 - 4d^- > 0$, with the curve $\overline{\Delta}(x, y) = 0$ (red). The part of the blue curve located in the fourth quadrant is the graph of Π. We draw $x = x^*$ and $y = x^*$ using dashed lines. $(x, y) = (x_C, -x_C)$ and $(x, y) = (-x_C, x_C)$ are the intersection points between the red curve and $y = -x$. We draw the contact point $(x, y) = (x_C, -x_C)$ when x_C is positive and contained in the domain of I (Fig. 7e) (Color figure online)

4. $(a_{11}^+ < 0)$ If $x^* = x_L$ (Fig. 7d), then $I < 0$ on $]0, x_L[$ and, for any small $\theta > 0$, $\mathrm{Cycl}(\cup_{x \in [\theta, x_L - \theta]} \Gamma_x) = 1$. The limit cycle is attracting.
5. $(a_{11}^+ < 0)$ If $\frac{1}{t^-} < x^* < x_L$ (Fig. 7e), then the function I has precisely 1 zero counting multiplicity on $]0, x^*[$ and, for any sufficiently small $\theta > 0$, $\mathrm{Cycl}(\cup_{x \in [\theta, x^* - \theta]} \Gamma_x) = 2$.
6. $(a_{11}^+ < 0)$ If $x^* = \frac{1}{t^-}$ (Fig. 7f), then $I > 0$ on $]0, x^*[$ and, for any small $\theta > 0$, $\mathrm{Cycl}(\cup_{x \in [\theta, x^* - \theta]} \Gamma_x) = 1$ (the limit cycle is repelling).
7. $(a_{11}^+ < 0)$ If $0 < x^* < \frac{1}{t^-}$ (Fig. 7g), then $I > 0$ on $]0, x^*[$ and, for any small $\theta > 0$, $\mathrm{Cycl}(\cup_{x \in [\theta, x^* - \theta]} \Gamma_x) = 1$ (the limit cycle is repelling).
8. $(a_{11}^+ > 0)$ If $x^* < 0$ (Fig. 7h), then $I < 0$ on $]0, \Pi^{-1}(x^*)[$ and, for any small $\theta > 0$, $\mathrm{Cycl}(\cup_{x \in [\theta, \Pi^{-1}(x^*) - \theta]} \Gamma_x) = 1$ (the limit cycle is attracting).
9. If $a_{11}^+ = 0$ (Fig. 7i), then we have $I < 0$ on $]0, x_L[$ and, for any small $\theta > 0$, $\mathrm{Cycl}(\cup_{x \in [\theta, x_L - \theta]} \Gamma_x) = 1$ (the limit cycle is attracting).

Proof Suppose that $d^- > 0$, $t^- > 0$ and $(t^-)^2 - 4d^- > 0$. From (20) it follows that

$$x_L = \frac{2}{t^- + \sqrt{(t^-)^2 - 4d^-}} > 0, \quad x_R = \frac{2}{t^- - \sqrt{(t^-)^2 - 4d^-}} > 0,$$

with $x_L < x_R$, $V(x_L) = V(x_R) = 0$ where $V(x) = d^- x^2 - t^- x + 1$. The graph of V is concave up ($d^- > 0$). It is not difficult to see that $\frac{1}{t^-} < x_L$. Using (38) $x_C \geq 0$ is well-defined if $x^* \geq \frac{1}{t^-}$.

Lemma 4.6 *Suppose that* $d^- > 0$, $t^- > 0$, $(t^-)^2 - 4d^- > 0$, $a_{11}^+ \neq 0$ *and* $V(x^*) \neq 0$ *(i.e.* $x^* \neq x_L, x_R$*). Then the following statements are true.*

1. *If* $x_R < x^*$, *then* $x_R < x_C < x^*$.
2. *If* $x_L < x^* < x_R$, *then* $x^* < x_C < x_R$.
3. *If* $\frac{1}{t^-} < x^* < x_L$, *then* $0 < x_C < x^*$.
4. *If* $x^* = \frac{1}{t^-}$, *then* $x_C = 0$.

Now, we prove the statements of Theorem 4.5.
Statement 1. Suppose that $x_R < x^*$. Then (32) and $V(x^*) > 0$ imply that $hp(0) > 0$ and $hp'(x) < 0$ for all $x \neq x^*$. The graph of hp is given in Fig. 7a.

Since $x_L < x_R < x^*$, the domain of I is $[0, x_L[$ (see Fig. 6a). It is clear (Fig. 7a) that the graph of hp lies above the graph of Π for $x \in]0, x_L[$ and Statement 2 of Lemma 4.2 implies that $I'(x) < 0$ for all $x \in]0, x_L[$. Hence, $I < 0$ on $]0, x_L[$. Following Statement 1 of Theorem 2.2, for any small $\theta > 0$, $\text{Cycl}(\cup_{x \in [\theta, x_L - \theta]} \Gamma_x) = 1$ (the limit cycle is attracting because I is negative).
Statement 2. Assume that $x^* = x_R$. The domain of I is $[0, x_L[$ (see the proof of Statement 1). Since $a_{11}^+ d^- \neq 0$ and $V(x^*) = 0$, $\overline{\Delta} = 0$ is the union of $x = x_R$ and $y = x_R$ (see Fig. 7b). The horizontal line $y = x_R$ lies above the graph of Π for $x \in]0, x_L[$, and Statement 2 of Lemma 4.2 implies that $I'(x) < 0$ for all $x \in]0, x_L[$. Thus, $I < 0$ on $]0, x_L[$. For any small $\theta > 0$, $\text{Cycl}(\cup_{x \in [\theta, x_L - \theta]} \Gamma_x) = 1$ (the limit cycle is attracting). See Statement 1 of Theorem 2.2.
Statement 3. Suppose that $x_L < x^* < x_R$. Then (32) and $V(x^*) < 0$ imply that $hp(0) > 0$ and $hp'(x) > 0$ for all $x \neq x^*$. The graph of hp is given in Fig. 7c. The proof of Statement 3 is similar to the proof of Statement 1.

Statement 4. Statement 4 can be proved in the same fashion as Statement 2 (see Fig. 7d).
Statement 5. Suppose that $\frac{1}{t^-} < x^* < x_L$. From (32) and $V(x^*) > 0$ it follows that $hp(0) > 0$ and $hp'(x) < 0$ for all $x \neq x^*$. The graph of hp is given in Fig. 7e. Statement 3 of Lemma 4.6 implies that the contact points between the orbits of system (34) and $y = hp(x)$ are $(x, y) = (x_L, x_R)$, $(x, y) = (x_R, x_L)$, $(x, y) = (x_C, -x_C)$ and $(x, y) = (-x_C, x_C)$, with $0 < x_C < x^*$.

The domain of I is $[0, x^*[$ (Fig. 6b). First we show that there is precisely 1 intersection (counting multiplicity) between the graph of hp and the graph of Π for $x \in]0, x^*[$. This will imply that I has at most 1 zero (counting multiplicity) on $]0, x^*[$ (see the proof of statement 3 of Theorem 4.3). Since $hp(0) > 0$, the graph of hp lies above the graph of Π for $x > 0$ and $x \sim 0$. Notice that $\Pi(x^*)$ is finite and that $hp(x) \to -\infty$ as

$x \rightarrow x^*-$. Thus, the graph of hp lies below the graph of Π for $x < x^*$ and $x \sim x^*$. We conclude that there exists at least 1 intersection between the graph of hp and the graph of Π for $x \in]0, x^*[$ (The Intermediate-Value Theorem). If we suppose that there exist at least 2 intersections (counting multiplicity), then, apart from $(x, y) = (x_C, -x_C)$, we have at least 1 extra contact point with the $x-$coordinate contained in $]0, x^*[$. This gives a contradiction. Thus, we have found precisely 1 intersection (counting multiplicity).

Now, we prove that I has a zero in $]0, x^*[$. Then the above discussion implies that I has precisely 1 zero counting multiplicity on $]0, x^*[$. Since the graph of hp lies above the graph of Π for $x > 0$ and $x \sim 0$, Lemma 4.2 (Statement 2) implies that $I'(x) < 0$ for $x > 0$ and $x \sim 0$. Hence, $I(x) < 0$ for $x > 0$ and $x \sim 0$. The integral in (15) can be written as

$$\int_{\Pi(x)}^{x} \frac{u \, du}{X^{sl}(u)} = \int_{\Pi(x)}^{0} \frac{u \, du}{X^{sl}(u)} + \int_{0}^{x} \frac{u \, du}{X^{sl}(u)}.$$

Since $\Pi(x^*) < 0$ (finite) and $x^* = -\frac{b^+ - a_{21}^+}{a_{11}^+} > 0$, the first component $\int_{\Pi(x)}^{0}$ tends to a negative number as $x \rightarrow x^*-$ (thus, it is bounded). It is clear that the second integral is divergent: $\int_{0}^{x} \rightarrow +\infty$ as $x \rightarrow x^*-$. This implies that I is positive for $x < x^*$ and $x \sim x^*$. From The Intermediate-Value Theorem it follows that I has a zero in $]0, x^*[$.

Now, Statement 3 of Theorem 2.2 implies that for any sufficiently small $\theta > 0$ we get $\text{Cycl}(\cup_{x \in [\theta, x^* - \theta]} \Gamma_x) = 2$.

Statement 6. Suppose that $x^* = \frac{1}{t^-}$. Then (32) and $V(x^*) > 0$ imply that $hp(0) = 0$ and $hp'(x) < 0$ for all $x \neq x^*$. The graph of hp is given in Fig. 7f. Using Statement 4 of Lemma 4.6, the contact points between the orbits of system (34) and $y = hp(x)$ are $(x, y) = (x_L, x_R)$, $(x, y) = (x_R, x_L)$ and $(x, y) = (0, 0)$.

The domain of I is $[0, x^*[$ (see the proof of Statement 5). We can prove that the graph of hp lies below the graph of Π for $x \in]0, x^*[$ using the same idea as in the proof of Theorem 4.3 (Statement 2). Then Statement 2 of Lemma 4.2 implies that $I > 0$ on $]0, x^*[$. Following Statement 1 of Theorem 2.2, for any small $\theta > 0$, $\text{Cycl}(\cup_{x \in [\theta, x^* - \theta]} \Gamma_x) = 1$ (the limit cycle is repelling).

Statement 7. Suppose that $0 < x^* < \frac{1}{t^-}$. Then we have $hp(0) < 0$ and $hp'(x) < 0$ for all $x \neq x^*$. The graph of hp is given in Fig. 7g. The contact points between the orbits of system (34) and $y = hp(x)$ are $(x, y) = (x_L, x_R)$ and $(x, y) = (x_R, x_L)$.

The domain of I is $[0, x^*[$ (see the proof of Statement 5). Again, we can show that the graph of hp lies below the graph of Π for $x \in]0, x^*[$ using the same technique as in the proof of Statement 1 of Theorem 4.3. Then Statement 2 of Lemma 4.2 implies that $I > 0$ on $]0, x^*[$. Using Statement 1 of Theorem 2.2, for any small $\theta > 0$, we get $\text{Cycl}(\cup_{x \in [\theta, x^* - \theta]} \Gamma_x) = 1$ (the limit cycle is repelling).

Statement 8. Suppose that $x^* < 0$. Then $hp(0) > 0$ and $hp'(x) < 0$ for all $x \neq x^*$. The graph of hp is given in Fig. 7h.

The domain of I is $[0, \Pi^{-1}(x^*)[$ (Fig. 6d). Clearly, the graph of hp lies above the graph of Π for $x \in]0, \Pi^{-1}(x^*)[$. Then Statement 2 of Lemma 4.2 implies that $I < 0$ on $]0, \Pi^{-1}(x^*)[$. Again, Statement 1 of Theorem 2.2 implies that for any small $\theta > 0$ $\text{Cycl}(\cup_{x \in [\theta, \Pi^{-1}(x^*) - \theta]} \Gamma_x) = 1$ (the limit cycle is attracting).
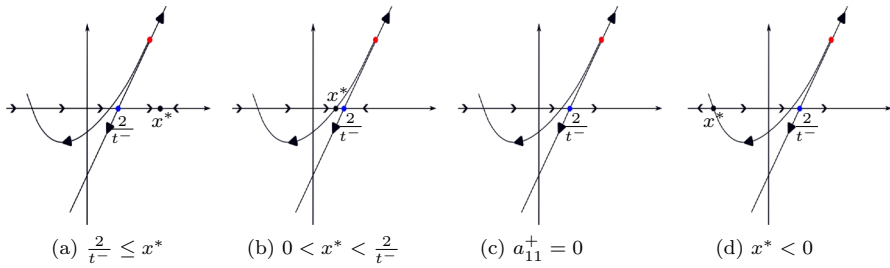
(a) $\frac{2}{t^-} \leq x^*$ (b) $0 < x^* < \frac{2}{t^-}$ (c) $a_{11}^+ = 0$ (d) $x^* < 0$

Fig. 8 Phase portraits of Z^- defined in (8) and the direction of the sliding vector field (11) along $y = 0$, with $t^- > 0$ and $(t^-)^2 - 4d^- = 0$. Z^- has a repelling node with repeated eigenvalues. We do not draw the corresponding phase portraits of Z^+

Statement 9. Assume that $a_{11}^+ = 0$. Recall that $d^- > 0$ and $t^- > 0$. The curve $\overline{\Delta} = 0$ is given by (33). We refer to Fig. 7i. The domain of I is $[0, x_L[$ (Fig. 6c). The graph of hp lies above the graph of Π for $x \in]0, x_L[$. This, together with Lemma 4.2 (Statement 2) and Theorem 2.2 (Statement 1), implies Statement 9.   □

4.3.2 Repeated Eigenvalues

In this section we assume that $d^- > 0$, $t^- > 0$ and $(t^-)^2 - 4d^- = 0$. System Z^- has a repelling node at $(x, y) = \left(\frac{4}{t^-}, \frac{4}{(t^-)^2} \right)$ with repeated eigenvalues $\varkappa_\pm = \frac{t^-}{2}$. The straight-line solution corresponding to the eigenvalue is given by $x = \frac{t^-}{2} y + \frac{2}{t^-}$. We refer to Lemma 2.3 and Fig. 8.

In this case the domain and image of Π are respectively $[0, \frac{2}{t^-}[$ and $] -\infty, 0]$ (see also [6]). We distinguish between 4 cases.

(a) If $a_{11}^+ < 0$ (hence $x^* > 0$) and $\frac{2}{t^-} \leq x^*$, then the domain of I is $[0, \frac{2}{t^-}[$ and we consider the canard cycle Γ_x for all $x \in]0, \frac{2}{t^-}[$ (see Fig. 8a).

(b) If $a_{11}^+ < 0$ and $x^* < \frac{2}{t^-}$, then the domain of I is $[0, x^*[$ and we consider the canard cycle Γ_x for all $x \in]0, x^*[$ (see Fig. 8b).

(c) If $a_{11}^+ = 0$, then we have the same domain of I as in the case (a) (see Fig. 8c).

(d) If $a_{11}^+ > 0$ (hence $x^* < 0$), then the domain of I is $[0, \Pi^{-1}(x^*)[$ and we consider the canard cycle Γ_x for all $x \in]0, \Pi^{-1}(x^*)[$ (see Fig. 8d).

System (34) has a hyperbolic saddle at the origin and a singularity at $(x, y) = \left(\frac{2}{t^-}, \frac{2}{t^-} \right)$ which is linearly zero (for more details see Fig. 9). The graph of the Poincaré half-map Π approaches the invariant line $x = \frac{2}{t^-}$.

Theorem 4.7 *Suppose that $d^- > 0$, $t^- > 0$ and $(t^-)^2 - 4d^- = 0$. Then the following statements are true.*

1. *($a_{11}^+ < 0$) If $\frac{2}{t^-} < x^*$ (Fig. 9a), then $I < 0$ on $]0, \frac{2}{t^-}[$ and, for any small $\theta > 0$, $\mathrm{Cycl}(\cup_{x \in [\theta, \frac{2}{t^-} - \theta]} \Gamma_x) = 1$ (the limit cycle is attracting).*

2. *($a_{11}^+ < 0$) If $x^* = \frac{2}{t^-}$ (Fig. 9b), then $I < 0$ on $]0, \frac{2}{t^-}[$ and, for any small $\theta > 0$, $\mathrm{Cycl}(\cup_{x \in [\theta, \frac{2}{t^-} - \theta]} \Gamma_x) = 1$ (the limit cycle is attracting).*

(a) $\frac{2}{t^-} < x^*$

(b) $x^* = \frac{2}{t^-}$

(c) $\frac{1}{t^-} < x^* < \frac{2}{t^-}$

(d) $x^* = \frac{1}{t^-}$

(e) $0 < x^* < \frac{1}{t^-}$

(f) $x^* < 0$

(g) $a_{11}^+ = 0$
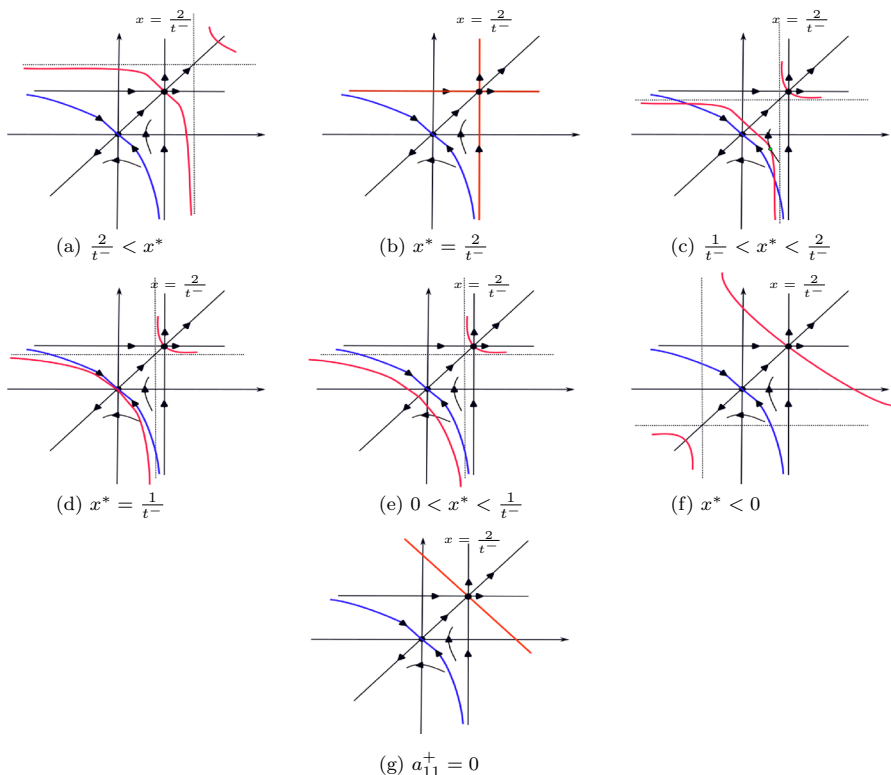
Fig. 9 The phase portrait of (34) for $d^- > 0$, $t^- > 0$ and $(t^-)^2 - 4d^- = 0$, with the curve $\overline{\Delta}(x, y) = 0$ (red). The part of the blue curve located in the fourth quadrant is the graph of Π. We draw $x = x^*$ and $y = x^*$ using dashed lines. We draw the contact point $(x, y) = (x_C, -x_C)$ when x_C is positive and contained in the domain of I (**c**) (Color figure online)

3. $(a_{11}^+ < 0)$ If $\frac{1}{t^-} < x^* < \frac{2}{t^-}$ (Fig. 9c), then the function I has precisely 1 zero counting multiplicity on $]0, x^*[$ and, for any sufficiently small $\theta > 0$, $\mathrm{Cycl}(\cup_{x\in[\theta, x^*-\theta]}\Gamma_x) = 2$.
4. $(a_{11}^+ < 0)$ If $x^* = \frac{1}{t^-}$ (Fig. 9d), then $I > 0$ on $]0, x^*[$ and, for any small $\theta > 0$, $\mathrm{Cycl}(\cup_{x\in[\theta, x^*-\theta]}\Gamma_x) = 1$ (the limit cycle is repelling).
5. $(a_{11}^+ < 0)$ If $0 < x^* < \frac{1}{t^-}$ (Fig. 9e), then $I > 0$ on $]0, x^*[$ and, for any small $\theta > 0$, $\mathrm{Cycl}(\cup_{x\in[\theta, x^*-\theta]}\Gamma_x) = 1$ (the limit cycle is repelling).
6. $(a_{11}^+ > 0)$ If $x^* < 0$ (Fig. 9f), then $I < 0$ on $]0, \Pi^{-1}(x^*)[$ and, for any small $\theta > 0$, $\mathrm{Cycl}(\cup_{x\in[\theta, \Pi^{-1}(x^*)-\theta]}\Gamma_x) = 1$ (the limit cycle is attracting).
7. If $a_{11}^+ = 0$ (Fig. 9g), then $I < 0$ on $]0, \frac{2}{t^-}[$ and, for any small $\theta > 0$, $\mathrm{Cycl}(\cup_{x\in[\theta, \frac{2}{t^-}-\theta]}\Gamma_x) = 1$ (the limit cycle is attracting).

Proof Let $d^- > 0$, $t^- > 0$ and $(t^-)^2 - 4d^- = 0$. From (20) it follows that $x_L = x_R = \frac{2}{t^-}$ and $V(\frac{2}{t^-}) = 0$. The graph of V is concave up and $V(x) > 0$ for all $x \neq \frac{2}{t^-}$. Using (38) and $(t^-)^2 - 4d^- = 0$ we have $x_C = \frac{2}{t^-}\sqrt{t^-x^* - 1}$.

Lemma 4.8 *Suppose that $d^- > 0$, $t^- > 0$, $(t^-)^2 - 4d^- = 0$, $a_{11}^+ \neq 0$ and $V(x^*) \neq 0$ (i.e. $x^* \neq \frac{2}{t^-}$). Then the following statements are true.*

1. *If $\frac{2}{t^-} < x^*$, then $\frac{2}{t^-} < x_C < x^*$.*
2. *If $\frac{1}{t^-} < x^* < \frac{2}{t^-}$, then $0 < x_C < x^*$.*
3. *If $x^* = \frac{1}{t^-}$, then $x_C = 0$.*

Now, we prove the statements of Theorem 4.7.

Statement 1. Suppose that $\frac{2}{t^-} < x^*$. From (32) it follows that $hp(0) > 0$ and $hp'(x) < 0$ for all $x \neq x^*$. The graph of hp is given in Fig. 9a. Since $\frac{2}{t^-} < x^*$, the domain of I is $[0, \frac{2}{t^-}[$ (see Fig. 8a). The proof now proceeds in a similar fashion to the proof of Statement 1 of Theorem 4.5.

Statement 2. Suppose that $x^* = \frac{2}{t^-}$. The domain of I is $[0, \frac{2}{t^-}[$ (see Fig. 8a). The proof of Statement 2 is similar to the proof of Theorem 4.5 (Statement 2) or Theorem 4.5 (Statement 4).

Statement 3. Suppose that $\frac{1}{t^-} < x^* < \frac{2}{t^-}$. From (32) it follows that $hp(0) > 0$ and $hp'(x) < 0$ for all $x \neq x^*$. The graph of hp is given in Fig. 9c. The domain of I is $[0, x^*[$ (see Fig. 8b). The proof is now analogous to the proof of Statement 5 of Theorem 4.5. Instead of Statement 3 of Lemma 4.6 3 we use Statement 2 of Lemma 4.8 and find the following contact points: $(x, y) = (\frac{2}{t^-}, \frac{2}{t^-})$, $(x, y) = (x_C, -x_C)$ and $(x, y) = (-x_C, x_C)$, with $0 < x_C < x^*$.

Statement 4. Suppose that $x^* = \frac{1}{t^-}$. We have $hp(0) = 0$ and $hp'(x) < 0$ for all $x \neq x^*$ (see Fig. 9d). The domain of I is $[0, x^*[$ (see Fig. 8b). The proof is similar to the proof of Statement 6 of Theorem 4.5. Using Statement 3 of Lemma 4.8 the contact points are $(x, y) = (\frac{2}{t^-}, \frac{2}{t^-})$ and $(x, y) = (0, 0)$.

Statement 5. Suppose that $0 < x^* < \frac{1}{t^-}$. We have $hp(0) < 0$ and $hp'(x) < 0$ for all $x \neq x^*$ (see Fig. 9e). The domain of I is $[0, x^*[$ (see Fig. 8b). The proof is similar to the proof of Statement 7 of Theorem 4.5. We have 1 contact point: $(x, y) = (\frac{2}{t^-}, \frac{2}{t^-})$.

Statement 6. Suppose that $x^* < 0$. We have $hp(0) > 0$ and $hp'(x) < 0$ for all $x \neq x^*$ (see Fig. 9f). The domain of I is $[0, \Pi^{-1}(x^*)[$ (see Fig. 8d). The proof is analogous to the proof of Statement 8 of Theorem 4.5.

Statement 7. Suppose that $a_{11}^+ = 0$. The curve $\overline{\Delta} = 0$ is given by (33): $y = \frac{4}{t^-} - x$. We refer to Fig. 9g. The domain of I is $[0, \frac{2}{t^-}[$ (Fig. 8c). The proof is analogous to the proof of Statement 9 of Theorem 4.5.   □

4.4 The Focus Case

Here we suppose that $d^- > 0$, $t^- > 0$ and $(t^-)^2 - 4d^- < 0$. System Z^- has a repelling focus at $(x, y) = (\frac{t^-}{d^-}, \frac{1}{d^-})$. We refer to Lemma 2.3 and Fig. 10. The domain and image of Π are respectively $[0, +\infty[$ and $] -\infty, 0]$ (see also [6]). The domain of the slow divergence integral I (or $\tilde{I}$) depends on x^* and we have 3 cases.

(a) If $a_{11}^+ < 0$ (hence $x^* > 0$), then the domain of I is $[0, x^*[$ and we consider the canard cycle Γ_x for all $x \in]0, x^*[$ (see Fig. 10a).
(b) If $a_{11}^+ = 0$, then the domain of I is $[0, +\infty[$ and we consider the canard cycle Γ_x for all $x \in]0, +\infty[$ (see Fig. 10b).
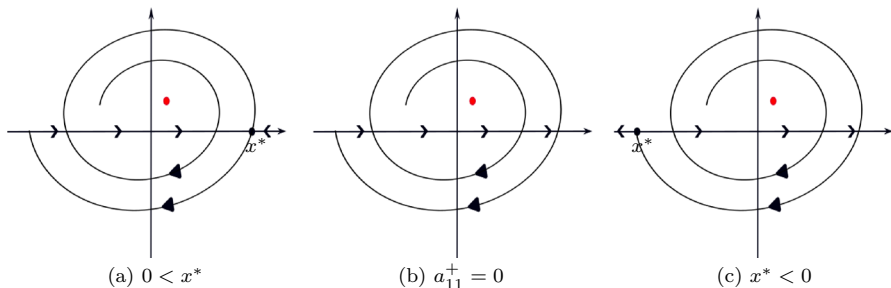
Fig. 10 Phase portraits of Z^- defined in (8) and the direction of the sliding vector field (11) along $y = 0$, for $d^- > 0, t^- > 0$ and $(t^-)^2 - 4d^- < 0$. Z^- has a repelling focus. We do not draw the corresponding phase portraits of Z^+
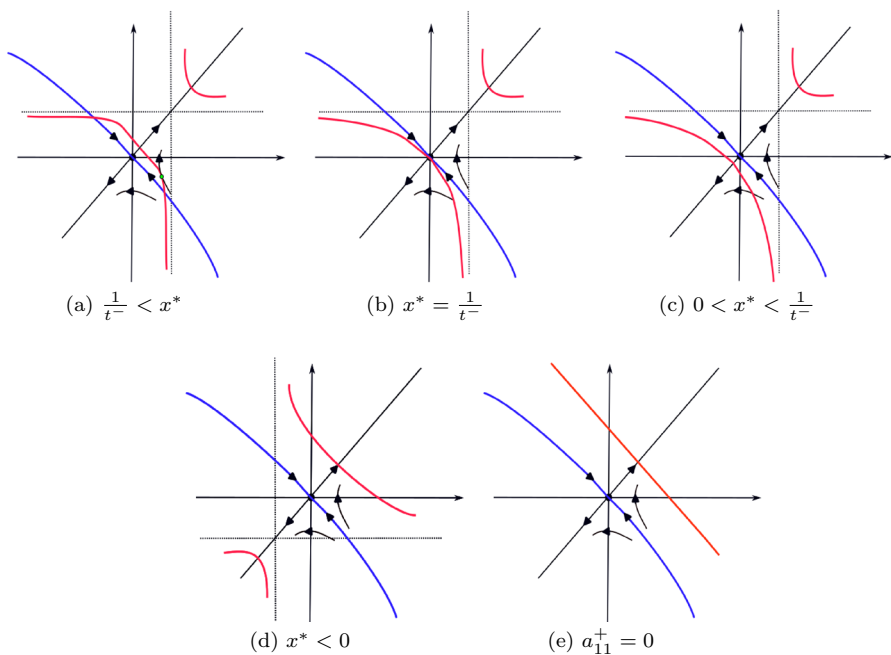

Fig. 11 The phase portrait of (34) for $d^- > 0, t^- > 0$ and $(t^-)^2 - 4d^- < 0$, with the curve $\overline{\Delta}(x, y) = 0$ (red). The part of the blue curve located in the fourth quadrant is the graph of Π. We draw $x = x^*$ and $y = x^*$ using dashed lines. We indicate the contact point $(x, y) = (x_C, -x_C)$ when x_C is positive and contained in the domain of I (**a**) (Color figure online)

(c) If $a_{11}^+ > 0$ (hence $x^* < 0$), then the domain of I is $[0, \Pi^{-1}(x^*)[$ and we consider the canard cycle Γ_x for all $x \in]0, \Pi^{-1}(x^*)[$ (see Fig. 10c).

System (34) has a hyperbolic saddle at the origin (Fig. 11).

Theorem 4.9 *Suppose that $d^- > 0$, $t^- > 0$ and $(t^-)^2 - 4d^- < 0$. Then the following statements are true.*

1. *($a_{11}^+ < 0$) If $\frac{1}{t^-} < x^*$ (Fig. 11a), then the function I has precisely 1 zero counting multiplicity on $]0, x^*[$ and, for any sufficiently small $\theta > 0$, $\mathrm{Cycl}(\cup_{x \in [\theta, x^* - \theta]} \Gamma_x) = 2$.*
2. *($a_{11}^+ < 0$) If $x^* = \frac{1}{t^-}$ (Fig. 11b), then $I > 0$ on $]0, x^*[$ and, for any small $\theta > 0$, $\mathrm{Cycl}(\cup_{x \in [\theta, x^* - \theta]} \Gamma_x) = 1$ (the limit cycle is repelling).*
3. *($a_{11}^+ < 0$) If $0 < x^* < \frac{1}{t^-}$ (Fig. 11c), then $I > 0$ on $]0, x^*[$ and, for any small $\theta > 0$, $\mathrm{Cycl}(\cup_{x \in [\theta, x^* - \theta]} \Gamma_x) = 1$ (the limit cycle is repelling).*
4. *($a_{11}^+ > 0$) If $x^* < 0$ (Fig. 11d), then $I < 0$ on $]0, \Pi^{-1}(x^*)[$ and, for any small $\theta > 0$, $\mathrm{Cycl}(\cup_{x \in [\theta, \Pi^{-1}(x^*) - \theta]} \Gamma_x) = 1$ (the limit cycle is attracting).*
5. *If $a_{11}^+ = 0$ (Fig. 11e), we have $I < 0$ on $]0, \infty[$ and, for any small $\theta > 0$, $\mathrm{Cycl}(\cup_{x \in [\theta, \frac{1}{\theta}]} \Gamma_x) = 1$ (the limit cycle is attracting).*

Proof We suppose that $d^- > 0$, $t^- > 0$ and $(t^-)^2 - 4d^- < 0$. Since $V(x) > 0$ for all $x \in \mathbb{R}$, then, for $a_{11}^+ \neq 0$, we have $hp'(x) < 0$ for all $x \neq x^*$ (see (32)). From (38) it follows that $x_C \geq 0$ is well-defined for $x^* \geq \frac{1}{t^-}$. If $x^* = \frac{1}{t^-}$, then $x_C = 0$, and, if $x^* > \frac{1}{t^-}$, then $0 < x_C < x^*$.

Statement 1. Suppose that $\frac{1}{t^-} < x^*$. From (32) it follows that $hp(0) > 0$. The graph of hp is given in Fig. 11a. The contact points between the orbits of system (34) and the hyperbola $y = hp(x)$ are $(x, y) = (x_C, -x_C)$ and $(x, y) = (-x_C, x_C)$, with $0 < x_C < x^*$. The domain of I is $[0, x^*[$ (see Fig. 10a). The proof is similar to the proof of Statement 5 of Theorem 4.5.

Statement 2. Suppose that $x^* = \frac{1}{t^-}$. We have $hp(0) = 0$ (see Fig. 11b). The domain of I is $[0, x^*[$ (see Fig. 10a). We have 1 contact point: $(x, y) = (0, 0)$. We can show that the graph of hp lies below the graph of Π for $x \in]0, x^*[$ using the same idea as in the proof of Statement 2 of Theorem 4.3. Then the result follows from Statement 2 of Lemma 4.2 and Statement 1 of Theorem 2.2.

Statement 3. Suppose that $0 < x^* < \frac{1}{t^-}$. We have $hp(0) < 0$. The graph of hp is given in Fig. 11c. There are no contact points between the orbits of system (34) and $y = hp(x)$.

The domain of I is $[0, x^*[$ (see Fig. 10a). Again, we can show that the graph of hp lies below the graph of Π for $x \in]0, x^*[$ using the same idea as in the proof of Statement 1 of Theorem 4.3. Then the result easily follows from Statement 2 of Lemma 4.2 and Statement 1 of Theorem 2.2.

Statement 4. Suppose that $x^* < 0$. Then $hp(0) > 0$ and the graph of hp is given in Fig. 11d. There are no contact points between the orbits of system (34) and $y = hp(x)$. The domain of I is $[0, \Pi^{-1}(x^*)[$ (Fig. 10c).

Let us prove that the graph of hp lies above the graph of Π for $x \in]0, \Pi^{-1}(x^*)[$. Suppose that there is an intersection between the graph of hp and the graph of Π for $x \in]0, \Pi^{-1}(x^*)[$. This implies the existence of a contact point between the orbits of system (34) and $y = hp(x)$. This gives a contradiction. Statement 4 follows now from Statement 2 of Lemma 4.2 and Statement 1 of Theorem 2.2.

Statement 5. Assume that $a_{11}^+ = 0$. The graph of (33) is given in Fig. 11e. There are no contact points between the orbits of system (34) and $y = hp(x)$ because the equation in (39) has no solutions. The domain of I is $[0, +\infty[$ (Fig. 10b). Again, we can show that the graph of hp lies above the graph of Π for $x \in]0, +\infty[$ (see the proof of Statement 4). Then Statement 2 of Lemma 4.2 and Statement 1 of Theorem 2.2 imply the result.   □

A The Center Case

We suppose that $d^- > 0$ and $t^- = 0$. System Z^- has a center at $(x, y) = (0, \frac{1}{d^-})$. We refer to Fig. 12. The domain and image of Π are respectively $[0, +\infty[$ and $] - \infty, 0]$. We have 3 cases.

(a) If $a_{11}^+ < 0$ (hence $x^* > 0$), then the domain of I is $[0, x^*[$ (see Fig. 12a). We have $I > 0$ on $]0, x^*[$, and, for any small $\theta > 0$, $\mathrm{Cycl}(\cup_{x \in [\theta, x^* - \theta]} \Gamma_x) = 1$. The limit cycle is repelling (Statement 2 of Theorem 4.1).

(b) If $a_{11}^+ = 0$, then the domain of I is $[0, +\infty[$ (see Fig. 12b). Since $(a_{11}^+, t^-) = (0, 0)$, we have $I \equiv 0$.

(c) If $a_{11}^+ > 0$ (hence $x^* < 0$), then the domain of I is $[0, \Pi^{-1}(x^*)[$ (see Fig. 12c). We have $I < 0$ on $]0, \Pi^{-1}(x^*)[$, and, for any small $\theta > 0$, $\mathrm{Cycl}(\cup_{x \in [\theta, \Pi^{-1}(x^*) - \theta]} \Gamma_x) = 1$ and the limit cycle is attracting (Statement 2 of Theorem 4.1).

Remark 7 When $d^- < 0$ and $t^- = 0$, system Z^- has a hyperbolic saddle at $(x, y) = (0, \frac{1}{d^-})$. In this case we can find the domain of I in the same way as in Sect. 4.2 (see Fig. 4) and then apply Statement 2 of Theorem 4.1 when $a_{11}^+ \neq 0$ (see the center case).
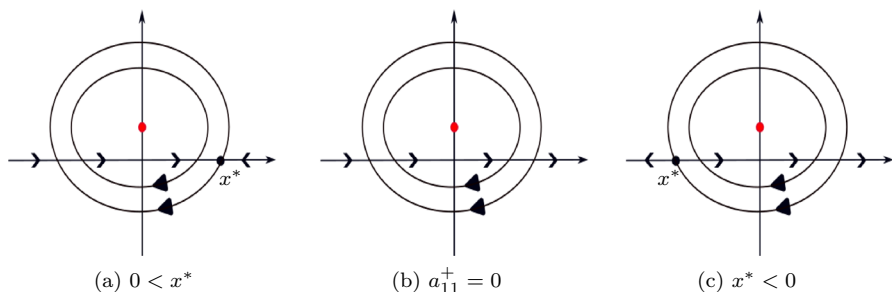

(a) $0 < x^*$ (b) $a_{11}^+ = 0$ (c) $x^* < 0$

Fig. 12 Phase portraits of Z^- defined in (8) and the direction of the sliding vector field (11) along $y = 0$, for $d^- > 0$ and $t^- = 0$. Z^- has a center. We do not draw the corresponding phase portraits of Z^+

B The Case Without Singularities

Here we suppose that $d^- = 0$ and $t^- \geq 0$. Then system Z^- has no singularities. If $t^- > 0$, then the line $x = t^- y + \frac{1}{t^-}$ is invariant w.r.t. Z^- (see Fig. 13a–d and Statement 3 of Lemma 2.3). The domain and image of Π are respectively $[0, \frac{1}{t^-}[$ and $] - \infty, 0]$. When $t^- = 0$, the domain and image of Π are respectively $[0, +\infty[$ and $] - \infty, 0]$. We refer to Fig. 13e–g.

We have

(a) If $t^- > 0$ and $\frac{1}{t^-} \leq x^*$, then the domain of I is $[0, \frac{1}{t^-}[$ (see Fig. 13a). When $\frac{1}{t^-} < x^*$, from Statement 1 of Theorem 4.1 it follows that $I < 0$ on $]0, \frac{1}{t^-}[$. For any small $\theta > 0$, $\text{Cycl}(\cup_{x \in [\theta, \frac{1}{t^-} - \theta]} \Gamma_x) = 1$ and the limit cycle is attracting. When $x^* = \frac{1}{t^-}$, then $I \equiv 0$.

(b) If $t^- > 0$ and $0 < x^* < \frac{1}{t^-}$, then the domain of I is $[0, x^*[$ (see Fig. 13b). Statement 1 of Theorem 4.1 implies that $I > 0$ on $]0, x^*[$, and, for any small $\theta > 0$, $\text{Cycl}(\cup_{x \in [\theta, x^* - \theta]} \Gamma_x) = 1$ (the limit cycle is repelling).

(c) If $t^- > 0$ and $a_{11}^+ = 0$, then we have the same domain of I as in the case (a) (see Fig. 13c). Again, Statement 1 of Theorem 4.1 implies that $I < 0$ on $]0, \frac{1}{t^-}[$.

(d) If $t^- > 0$ and $x^* < 0$, then the domain of I is $[0, \Pi^{-1}(x^*)[$ (see Fig. 13d). We have $I < 0$ on $]0, \Pi^{-1}(x^*)[$ and, for any small $\theta > 0$, we have $\text{Cycl}(\cup_{x \in [\theta, \Pi^{-1}(x^*) - \theta]} \Gamma_x) = 1$ and the limit cycle is attracting (Statement 1 of Theorem 4.1).

(e) If $t^- = 0$ and $0 < x^*$, then the domain of I is $[0, x^*[$ (see Fig. 13e). We have $I > 0$ on $]0, x^*[$, and, for any small $\theta > 0$, $\text{Cycl}(\cup_{x \in [\theta, x^* - \theta]} \Gamma_x) = 1$ and the limit cycle is repelling (Statement 1 of Theorem 4.1).
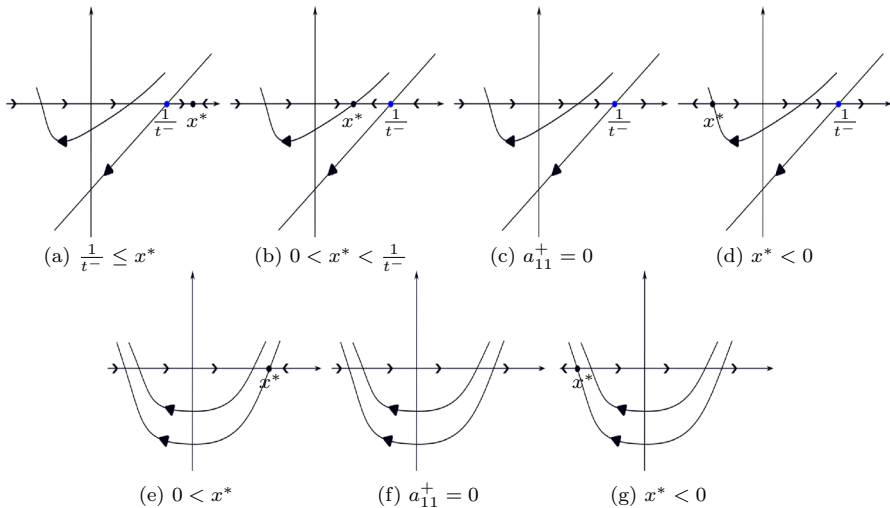

(a) $\frac{1}{t^-} \leq x^*$ (b) $0 < x^* < \frac{1}{t^-}$ (c) $a_{11}^+ = 0$ (d) $x^* < 0$

(e) $0 < x^*$ (f) $a_{11}^+ = 0$ (g) $x^* < 0$

Fig. 13 Phase portraits of Z^-, with $d^- = 0$, defined in (8) and the direction of the sliding vector field (11) along $y = 0$. **a–d** $t^- > 0$. **e–g** $t^- = 0$. We do not draw the corresponding phase portraits of Z^+

(f) If $t^- = 0$ and $a_{11}^+ = 0$, then the domain of I is $[0, +\infty[$ (see Fig. 13f). We have $I \equiv 0$.

(g) If $t^- = 0$ and $x^* < 0$, then the domain of I is $[0, \Pi^{-1}(x^*)[$ (see Fig. 13g). We have the same sign of I as in the case (d).

Declarations

Conflict of interest The authors declare that they have no conflict of interest.

Ethical Approval Not applicable.

References

1. Álvarez, M.J., Coll, B., De Maesschalck, P., Prohens, R.: Asymptotic lower bounds on Hilbert numbers using canard cycles. J. Differ. Equ. **268**(7), 3370–3391 (2020)
2. Berger, E.J.: Friction modeling for dynamic system simulation. Appl. Mech. Rev. **55**(6), 535–577 (2002)
3. Bonet-Reves, C., Larrosa, J., M-Seara, T.: Regularization around a generic codimension one fold–fold singularity. J. Differ. Equ. **265**(5), 1761–1838 (2018)
4. Bossolini, E., Brøns, M., Kristiansen, K.U.: A stiction oscillator with canards: on piecewise smooth nonuniqueness and its resolution by regularization using geometric singular perturbation theory. SIAM Rev. **62**(4), 869–897 (2020)
5. Braga, D.C., Mello, L.F.: Limit cycles in a family of discontinuous piecewise linear differential systems with two zones in the plane. Nonlinear Dyn. **73**(3), 1283–1288 (2013)
6. Carmona, V., Fernández-Sánchez, F.: Integral characterization for Poincaré half-maps in planar linear systems. J. Differ. Equ. **305**, 319–346 (2021)
7. Carmona, V., Fernández-Sánchez, F., Garcia-Medina, E., Novaes, D.: Properties of Poincaré half-maps for planar linear systems and some direct applications to periodic orbits of piecewise systems. Electron. J. Qual. Theory Differ. Equ. **2023**, 18 (2023)
8. Carmona, V., Fernández-Sánchez, F., Novaes, D.D.: A succinct characterization of period annuli in planar piecewise linear differential systems with a straight line of nonsmoothness. J. Nonlinear Sci. **33**(5), 13 (2023)

9. Carmona, V., Fernández-Sánchez, F., Novaes, D.D.: Uniform upper bound for the number of limit cycles of planar piecewise linear differential systems with two zones separated by a straight line. Appl. Math. Lett. **137**, 108501 (2023)

10. Carmona, V., Fernández-Sánchez, F., Novaes, D.D.: Uniqueness and stability of limit cycles in planar piecewise linear differential systems without sliding region. Commun. Nonlinear Sci. Numer. Simul. **123**, 18 (2023)

11. Carmona, V., Fernández-Sánchez, Fernando, Novaes, D.D.: A new simple proof for Lum–Chua's conjecture. Nonlinear Anal. Hybrid Syst. **40**, 100992 (2021)

12. Caubergh, M.: Hilbert's sixteenth problem for polynomial Liénard equations. Qual. Theory Dyn. Syst. **11**(1), 3–18 (2012)

13. Cheesman, N.D., Hogan, S.J., Uldall Kristiansen, K.: The Painlevé paradox in three dimensions: resolution with regularization. Proc. R. Soc. A: Math. Phys. Eng. Sci. **479**(2280), 20230419 (2023)

14. De Maesschalck, P., Dumortier, F.: Time analysis and entry–exit relation near planar turning points. J. Differ. Equ. **215**(2), 225–267 (2005)

15. De Maesschalck, P., Dumortier, F.: Canard cycles in the presence of slow dynamics with singularities. Proc. R. Soc. Edinb. Sect. A **138**(2), 265–299 (2008)

16. De Maesschalck, P., Dumortier, F., Roussarie, R.: Canard cycles—from birth to transition, volume 73 of Ergebnisse der Mathematik und ihrer Grenzgebiete. 3. Folge. A Series of Modern Surveys in Mathematics [Results in Mathematics and Related Areas. 3rd Series. A Series of Modern Surveys in Mathematics]. Springer, Cham (2021)

17. De Maesschalck, P., Huzak, R.: Slow divergence integrals in classical Liénard equations near centers. J. Dyn. Differ. Equ. **27**(1), 177–185 (2015)

18. di Bernardo, M., Budd, C.J., Champneys, A.R., Kowalczyk, P.: Piecewise-Smooth Dynamical Systems: Theory and Applications. Springer, London (2008)

19. Dumortier, F., Panazzolo, D., Roussarie, R.: More limit cycles than expected in Liénard equations. Proc. Am. Math. Soc. **135**(6), 1895–1904 (2007)

20. Dumortier, F., Roussarie, F.: Canard cycles and center manifolds. Mem. Am. Math. Soc. **121**(577), x+100 (1996). (**With an appendix by Cheng Zhi Li**)

21. Dumortier, F., Roussarie, R.: Canard cycles with two breaking parameters. Discrete Contin. Dyn. Syst. **17**(4), 787–806 (2007)

22. Dumortier, F., Roussarie, R., Rousseau, C.: Hilbert's 16th problem for quadratic vector fields. J. Differ. Equ. **110**(1), 86–133 (1994)

23. Esteban, M., Llibre, J., Valls, C.: The 16th Hilbert problem for discontinuous piecewise isochronous centers of degree one or two separated by a straight line. Chaos **31**(4), 043112 (2021)

24. Filippov, A.F.: Differential Equations with Discontinuous Righthand Sides. Mathematics and its Applications, Kluwer Academic Publishers, Norwell (1988)

25. Freire, E., Ponce, E., Rodrigo, F., Torres, F.: Bifurcation sets of continuous piecewise linear systems with two zones. Int. J. Bifurc. Chaos Appl. Sci. Eng. **8**(11), 2073–2097 (1998)

26. Freire, E., Ponce, E., Torres, F.: Canonical discontinuous planar piecewise linear systems. SIAM J. Appl. Dyn. Syst. **11**(1), 181–211 (2012)

27. Freire, E., Ponce, E., Torres, F.: Planar filippov systems with maximal crossing set and piecewise linear focus dynamics. Springer Proc. Math. Stat. **54**, 221–232 (2013)

28. Gasull, A., Torregrosa, J., Zhang, X.: Piecewise linear differential systems with an algebraic line of separation. Electron. J. Differ. Equ. **2020**, 14 (2020)

29. Guardia, M., Seara, T.M., Teixeira, M.A.: Generic bifurcations of low codimension of planar Filippov systems. J. Differ. Equ. **250**(4), 1967–2023 (2011)

30. Han, M., Zhang, W.: On Hopf bifurcation in non-smooth planar systems. J. Differ. Equ. **248**(9), 2399–2416 (2010)

31. Huan, S.M., Yang, X.S.: On the number of limit cycles in general planar piecewise linear systems. Discrete Contin. Dyn. Syst. **32**(6), 2147–2164 (2012)

32. Huan, S.M., Yang, X.S.: Existence of limit cycles in general planar piecewise linear systems of saddle–saddle dynamics. Nonlinear Anal. Theory Methods Appl. Ser. A Theory Methods **92**, 82–95 (2013)

33. Huan, S.M., Yang, X.S.: On the number of limit cycles in general planar piecewise linear systems of node–node types. J. Math. Anal. Appl. **411**(1), 340–353 (2014)

34. Huzak, R., De Maesschalck, P., Dumortier, F.: Limit cycles in slow–fast codimension 3 saddle and elliptic bifurcations. J. Differ. Equ. **255**(11), 4012–4051 (2013)

35. Huzak, R., Uldall Kristiansen, K.: General results on sliding cycles in regularized piecewise linear systems (in progress)
36. Huzak, R., Uldall Kristiansen, K.: The number of limit cycles for regularized piecewise polynomial systems is unbounded. J. Differ. Equ. **342**, 34–62 (2023)
37. Huzak, R., Uldall Kristiansen, K., Radunović, G.: Slow divergence integral in regularized piecewise smooth systems (2023). (submitted)
38. Jelbart, S., Kristiansen, K.U., Wechselberger, M.: Singularly perturbed boundary-equilibrium bifurcations. Nonlinearity **34**(11), 7371–7414 (2021)
39. Jelbart, S., Kristiansen, K.U., Wechselberger, M.: Singularly perturbed boundary-focus bifurcations. J. Differ. Equ. **296**, 412–492 (2021)
40. Kristiansen, K.U., Hogan, S.J.: Resolution of the piecewise smooth visible–invisible two-fold singularity in R3 using regularization and blowup. J. Nonlinear Sci. **29**(2), 723–787 (2018)
41. Kristiansen, K.U.: The regularized visible fold revisited. J. Nonlinear Sci. **30**(6), 2463–2511 (2020)
42. Kristiansen, K.U., Hogan, S.J.: Regularizations of two-fold bifurcations in planar piecewise smooth systems using blowup. SIAM J. Appl. Dyn. Syst. **14**(4), 1731–1786 (2015)
43. Krupa, M., Szmolyan, P.: Relaxation oscillation and canard explosion. J. Differ. Equ. **174**(2), 312–368 (2001)
44. Kuznetsov, Yu.A., Rinaldi, S., Gragnani, A.: One parameter bifurcations in planar Filippov systems. Int. J. Bifurc. Chaos **13**, 2157–2188 (2003)
45. Li, S., Liu, S., Llibre, J.: The planar discontinuous piecewise linear refracting systems have at most one limit cycle. Nonlinear Anal. Hybrid Syst. **41**, 14 (2021)
46. Li, S., Llibre, J.: Phase portraits of planar piecewise linear refracting systems: focus-saddle case. Nonlinear Anal. Real World Appl. **56**, 11 (2020)
47. Li, T., Llibre, J.: On the 16th Hilbert problem for discontinuous piecewise polynomial Hamiltonian systems. J. Dyn. Differ. Equ. **35**, 1–16 (2021)
48. Llibre, J., Ordóñez, M., Ponce, E.: On the existence and uniqueness of limit cycles in planar continuous piecewise linear systems without symmetry. Nonlinear Anal. Real World Appl. **14**(5), 2002–2012 (2013)
49. Llibre, J., Ponce, E.: Three nested limit cycles in discontinuous piecewise linear differential systems with two zones. Dyn. Contin. Discrete Impuls. Syst. Ser. B, Appl. Algorithms **19**(3), 325–335 (2012)
50. Llibre, J., Teixeira, M.A., Torregrosa, J.: Lower bounds for the maximum number of limit cycles of discontinuous piecewise linear differential systems with a straight line of separation. Int. J. Bifurc. Chaos **23**(4), 1350066 (2013)
51. Llibre, J., Teruel, A.E.: Introduction to the Qualitative Theory of Differential Systems. Planar, Symmetric and Continuous Piecewise Linear Systems. Birkhäuser Advanced Texts Basler Lehrbüch, Birkhäuser/Springer, Basel (2014)
52. Lum, R.: Global properties of continuous piecewise linear vector-fields. 1. Simplest case in r2. Int. J. Circuit Theory Appl. **19**(3), 251–307 (1991)
53. Medrado, J.C., Torregrosa, J.: Uniqueness of limit cycles for sewing planar piecewise linear systems. J. Math. Anal. Appl. **431**(1), 529–544 (2015)
54. Simpson, D.J.W.: A general framework for boundary equilibrium bifurcations of Filippov systems. Chaos **28**(10), 103114 (2018)
55. Smale, S.: Mathematical problems for the next century. In: Mathematics: Frontiers and Perspectives, pp. 271–294. American Mathematical Society, Providence (2000)
56. Sotomayor, J., Teixeira, M.A.: Regularization of discontinuous vector fields. In: Proceedings of the International Conference on Differential Equations, Lisboa, pp. 207–223 (1996)